Quantitative mapping of mRNA 3' ends in *Pseudomonas aeruginosa* reveals putative riboregulators and a pervasive role for transcription termination in response to azithromycin

Salini Konikkat[1], Michelle R. Scribner[2], Rory Eutsey[1], N. Luisa Hiller[1], Vaughn S. Cooper[2], C. Joel McManus[1]
[1] Department of Biological Sciences, Carnegie Mellon University, Pittsburgh, USA;
[2]Department of Microbiology and Molecular Genetics, University of Pittsburgh, Pittsburgh, USA

ABSTRACT

P. aeruginosa produces serious chronic infections in hospitalized patients and immunocompromised individuals, including cystic fibrosis patients. The molecular mechanisms by which *P. aeruginosa* responds to antibiotics and other stresses to promote persistent infections may provide new avenues for therapeutic intervention. Azithromycin (AZM), an antibiotic frequently used in cystic fibrosis treatment, is thought to improve clinical outcomes through a number of mechanisms including impaired biofilm growth and QS. The mechanisms underlying the transcriptional response to AZM remain unclear. Here, we interrogated the *P. aeruginosa* transcriptional response to AZM using an improved genome-wide approach to quantitate RNA 3'-ends (3pMap). We also identified hundreds of *P. aeruginosa* genes subject to premature transcription termination in their transcript leaders using 3pMap. AZM treatment of planktonic and biofilm cultures alters the expression of hundreds of genes, including those involved in QS, biofilm formation, and virulence. Strikingly, most genes downregulated by AZM in biofilms had increased levels of intragenic 3'-ends indicating premature transcription termination or pausing. Reciprocally, AZM reduced premature transcription termination in many upregulated genes. Most notably, reduced termination accompanied robust induction of *obgE*, a GTPase involved in persister formation in *P. aeruginosa*. Our results support a model in which AZM-induced premature transcription termination downregulates expression of central transcriptional regulators, which in turn both impairs QS and biofilm formation, and stress responses, while upregulating genes associated with persistence.

INTRODUCTION

The gram-negative bacterium *Pseudomonas aeruginosa* (*P. aeruginosa*) is a common cause of opportunistic infections, particularly in hospitalized patients [1-3]. It is a leading cause of ventilator-associated pneumonia and multi-drug resistant infections in intensive care units [4]. *P. aeruginosa* infects a wide range of human tissues including the lungs, urinary tract, skin, ear, eyes, and intestine, and is associated with increased morbidity and risk of death in immunocompromised patients with cystic fibrosis, chronic obstructive pulmonary disease (COPD), chronic wounds, burns, and cancer [2, 3, 5,6]. Over the past two decades, multidrug-resistant *P. aeruginosa* infections have been on the rise, and it is among the top three killers on World Health Organizations' 'dirty dozen' list of emerging antibiotic-resistant human pathogens [7-9].

Bacteria often employ conditional transcription termination in their transcript leaders to regulate expression in response to drugs, metabolites, and stresses [10-16]. *Cis*-regulatory elements that use premature transcription termination include transcription attenuators and riboswitches, often collectively referred to as riboregulators. Their mechanisms of action involve formation of alternate RNA structures that promote full length transcript synthesis (anti-terminator) or effect premature transcription termination (terminator). Alternate structure formation is mediated by interaction of the nascent transcript with small molecules, ribosomes, tRNAs, or regulatory proteins. As such, riboregulators are potential therapeutic targets, and may provide synthetic biology applications [17-20]. Since conditional premature transcription termination regulates biofilm formation, virulence, and expression of antibiotic resistance genes in other bacteria [21-24], it would be beneficial to identify and characterize genes controlled by riboregulators in *P. aeruginosa.*

P. aeruginosa readily forms aggregates or biofilms, in which bacterial cells are held together by a structural scaffold of extracellular polymeric substances comprised of exopolysaccharides, extracellular DNA, and polypeptides [9,25]**.** Biofilm growth is thought to exacerbate disease progression, and contributes to antibiotic resistance and the persistent nature of *P. aeruginosa* infections [26-29]. For example, in the lungs of cystic fibrosis patients, *P. aeruginosa* biofilms cause continual damage to the airways by recurrent infection, inflammation, and airway obstruction [30]. Due to their clinical importance, understanding the regulation of biofilms has become a major focus of *P. aeruginosa* research.

Sub-inhibitory concentrations of the macrolide antibiotic azithromycin (AZM) improves clinical outcomes in patients with cystic fibrosis, diffuse panbronchiolitis (DPB) and chronic obstructive pulmonary disease (COPD) [31-35]**.** In mouse models of *P. aeruginosa* infection, including a CF model, AZM reduced bacterial load and improved lung pathology [36,37]. These effects were attributed to the interference with quorum sensing (QS), the release of virulence factors*,* and attenuation of host inflammatory responses. Previous studies demonstrated that AZM targets QS by an uncertain mechanism, which in turn is proposed to control biofilm formation and virulence factor production [38-48]**.** Consistent with these biological effects, AZM treatment changes the transcript levels of genes involved in QS, virulence factor production, and oxidative stress [2,39-48]**.** For example, AZM downregulates the expression of components of the *lasI/lasR* and *rhlI/rhlR* QS systems as well as QS-controlled genes coding for virulence factors such as elastase, flagellar motility factors, and rhamnolipid synthesis [2,6,20,39,42,43,45-48]**.** AZM also downregulates QS-regulated oxidative stress response genes including catalase *katA* and superoxide dismutase *sodB* [49]**.** While these pathways clearly respond to AZM, the underlying mechanisms remain unclear, particularly in biofilms.

AZM binds near the peptidyl transferase center on the large subunit of bacterial ribosomes and disrupts translation elongation by hindering the passage of newly synthesized polypeptides through the polypeptide exit tunnel [50-54]**.** Translation inhibition is hence thought to account for QS inhibition, which in turn inhibits biofilm formation and virulence gene expression by AZM in *P. aeruginosa*. Because transcription elongation and mRNA translation are spatio-temporally coupled in bacteria [55-57], the translation stalling caused by AZM could directly alter the production of full-length transcripts from QS genes and transcriptional regulators of the stress response. The extent of reduced transcriptional processivity due to AZM treatment remains an important unresolved question because methods used in previous studies lacked the resolution to differentiate between premature and full-length mRNA transcripts.

RNA 3'-end mapping can reveal genes affected by premature transcription termination. Term-Seq, a recently developed high-throughput sequencing approach, allows genome-wide identification of RNA 3'-OH ends (subsequently referred to as 3'-end) [22]. In addition, differential expression changes can be quantified from transcriptome-wide 3'-end mapping [58-60]. In this study, we employed a modification of Term-Seq, called 3pMap (Figure 1), to characterize the transcriptional landscape of *P. aeruginosa* and the acute effects of clinically

relevant sub-inhibitory concentrations of AZM on gene expression. 3pMap identified hundreds of genes putatively controlled by riboregulators in *P. aeruginosa*, many of which may be new therapeutic targets. We further examined differential gene expression in planktonic and biofilm cultures of *P. aeruginosa* in response to AZM. AZM altered the expression of over two hundred genes in each condition, including key factors involved in QS, biofilm formation, virulence factor production, and stress responses. Notably, most genes downregulated in response to AZM in biofilms showed increased premature transcription termination, indicating a role for the antibiotic in regulating transcription. Furthermore, AZM treatment strongly induced the perister gene *obgE* [61], accompanied by a corresponding decrease in premature transcription termination in its transcript leader. Together, our results provide novel insights into transcriptional regulation in *P. aeruginosa*, and support a model in which AZM-induced premature termination alters the expression of key transcriptional modulators and structural genes involved in QS, virulence, stress response, and persistence.

METHODS

Strains and culture conditions

The effects of AZM on both planktonic cells and biofilms of *P. aeruginosa* strain PA14 were investigated. Populations from freezer stock were revived by culturing overnight in LB broth at 37°C with shaking at 300 RPM to an optical density (OD_{600}) of 1.0. For planktonic cells, this culture was diluted to OD_{600} 0.1 in 5 mL LB broth and grown to a final OD_{600} of 0.47 (approximately 3 hours shaking at 37C). A subinhibitory concentration of AZM (0.5 µg/ml final concentration) was added to three cultures (Supplementary Figure 1). Three cultures without AZM were used as negative controls. The cultures were incubated for an additional 20 minutes at 37°C. One volume of RNA stabilization solution (5.3M ammonium sulfate, 20 mM EDTA, 25 mM sodium citrate, pH 5.2) was added and the cells were pelleted by centrifugation at 2,500g for 10 minutes. The supernatants were discarded and the pellets were frozen at -20°C for RNA extraction. For biofilms, a mid-log phase PA14 culture was diluted to an optical density of 0.05 into six-well plates (one plate per culture) incubated at 37°C for 24 hours. The media was removed and replaced with or without AZM (0.5 µg/ml) and incubated at 37°C for 3 hours. The media was removed and 750 ul RNA stabilization solution was added to each well. The biofilms were scraped from the wells and the cells

were pelleted by centrifugation at 2500xG for 10 minutes. The supernatants were discarded and samples were saved at -20°C until RNA extraction.

RNA extraction and DNase treatment

Total RNA was extracted using the Quick-RNA™ Fungal/Bacterial Miniprep kit (Zymo Research R2010) according to the manufacturer's instructions. To remove any contaminating genomic DNA, 20-40 mg of total RNA was incubated with 6 units of TURBO^{TM}-DNase (Thermo Fisher Scientific AM2238), 1X TURBO^{TM}DNase buffer, and 20 units of SUPERase-In^{TM}RNase inhibitor in a 1 ml reaction for 1 hour at 37°C.The RNA was re-isolated using acid-phenol, ethanol precipitated, and resuspended in nuclease free water. The absence of contaminating DNA was confirmed by the absence of a GAPDH PCR product, using genomic DNA as a positive control for the PCR.

HIGH-THROUGHPUT SEQUENCING LIBRARY PREPARATION USING 3PMAP

3'-linker addition and rRNA depletion

To reduce secondary structure, a 5 µl reaction containing 2 µg of RNA and 375 ng of universal miRNA 3'-cloning linker (New England Biolabs S1315S) was heated at 80°C for 2 minutes and placed on ice. The RNA was ligated to the 3'-linker by incubating the mix overnight at 16°C in a 20 µl reaction containing 12.5 % PEG800, 10% DMSO, 1X T4 RNA Ligase buffer, 20 units SUPERase-In RNase inhibitor, and 200 units of T4 RNA Ligase 2, truncated K227Q (New England Biolabs M0351S). The RNA was precipitated with 3 volumes of ethanol, 1/10thvolume of 3M sodium acetate (pH 5.2) and 20 µg of glycogen at -80°C for 1 hour. Ribosomal RNA (rRNA) depletion was performed using the Ribo-Zero rRNA removal kit for bacteria (Illumina MRZMB126) as per the manufacturer's instructions, and ethanol precipitated as discussed above.

High-throughput sequencing library synthesis and sequencing

Strand-specific 3pMap libraries were prepared using the QuantSeq Flex Targeted RNA-seq kit (Lexogen SKU:035.24) with the following modifications. Primers used for library synthesis are listed below. First strand cDNA synthesis was performed as per the manufacturer's instruction using 5 µl of 2.5 µM custom first strand synthesis primer mix containing partial Illumina Read 1 adapter (below). Following the first strand synthesis, RNA was removed, and the second strand of cDNA was synthesized using SS1X mix and custom second strand synthesis primer with Illumina Read 2 sequence. Half the purified

cDNA was used as a template for PCR amplification using barcoded primers provided with the kit. The library concentrations were quantified using a Qubit dsDNA high sensitivity assay (ThermoFisher Scientific Q32854) and sizes were estimated on a Tapestation high sensitivity DNA ScreenTape (Aglient). The libraries were sequenced on an Illumina NextSeq 500 platform in a single-read, 75-nucleotide run.

OLIGONUCLEOTIDES FOR LIBRARY PREPARATION

First Strand Synthesis Mix (equimolar mix of three primers used for first strand synthesis):

3PUTR-FS-N-Read1 5'-CACGACGCTCTTCCGATCTNATTGATGGTGCCTACAG-3'

3PUTR-FS-NN-Read1 5'-CACGACGCTCTTCCGATCTNNATTGATGGTGCCTACAG-3'

3PUTR-FS-NNN-Read1 5'-CACGACGCTCTTCCGATCTNNNATTGATGGTGCCTACAG-3'

Random Second Strand Synthesis (SS) Primer

RandomSS-Read2 5'-GTTCAGACGTGTGCTCTTCCGATCTNNNNNNNNNNNN-3'

DATA PROCESSING

Aligning reads to the genome and identifying significant peaks

Raw sequencing reads were adapter trimmed using cutadapt (v. 1.9.1; parameters -a AGATCGGAAGAGC -m 25) and aligned to the UCBP-PA14 reference genome (NCBI) using Bowtie2 (v 2.1.0, default parameters) [62,63]. 3pMap is strand specific, such that reads map to the strand from which they were transcribed. We used a custom Perl script, Map3p-seq-peaks.pl, to compare aligned 3'-end locations to an expected Poisson distribution of random 3'-ends in 50 nucleotide windows. Candidate peaks required a raw p-value < 5 x 10^-5, > 5-fold more reads than the average within the window, and a minimum of 5 total reads per peak. RNA 3'-peaks that are present in at least two of three sample replicates were identified using a combination of bedtools functions [64] and custom Python scripts. These peaks are referred to as significant peaks in further analyses.

Genome-browser images

Integrated Genome Viewer [65] (IGV) images were exported as Scaled Vector Graphics (.svg) images and edited on Adobe Illustrator to obtain simplified views. Views for negative strand genes were inverted using mirror display option for ease of visualization. IGV tracks show the reads present in the same strand as the gene of interest.

Associating 3'-end reads with *P. aeruginosa* genes

Genomic coordinates of transcript leaders (5'-UTRs) were obtained using LiftOver (UCSC genome browser) from a previous study on the PAO1 strain [66, 67] (Supplementary Table 7). If the lifted-over transcript leaders encroached the CDS of an upstream PA14 gene, gene boundaries in the PA14 genome annotation were retained. 3'-end reads within 400 nucleotides of genes were identified using the bedtools windowbed function. The 3'-end reads were assigned to gene 3' UTR regions if they satisfied either of the following conditions: a) the read is within defined gene transcript boundaries, b) read is downstream of the annotated 3'-end of a gene and does not overlap more than 10 nucleotides into the next gene.

Predicting genes regulated by transcription termination in *P. aeruginosa* transcript leaders

We categorized reads present in the transcript leaders or 0-40 nucleotides into the ORF as early transcription termination events (Early termination reads). Percentage early termination reads (%ET) was calculated as follows:

$$\% \text{ ET} = (\text{Early termination reads} / \text{Total 3'-reads in the gene}) * 100$$

Highest % ET that detected most predicted/known riboswitches (Supplementary Table S1) in *P. aeruginosa* was employed as cut-off (Supplementary Figure 3A). Genes with % ET above the cut-off in at least two replicates were considered for the next step. Since significant peaks denote termination sites that are reproducibly present above background noise in at least two replicates, only genes with significant peaks in their early termination zone were considered as early termination or attenuation candidates. The ability of the RNA sequence upstream of significant peaks to form alternate RNA structures was analyzed using the PASIFIC (Prediction of Alternative Structures for Identification of cis-regulation) web-based application [68]. Sequences were analyzed for the ability to form Rho-independent (intrinsic) terminators using ARNold [69].

Quantifying the effects of AZM on gene expression in *P. aeruginosa*

Not all expressed genes had 3'-end peaks showing the location of full-length transcript termination. For differential expression, we used total read counts in the 3'-UTR regions of genes (all 3'-reads). These were compiled using a custom Python script, and pairwise differential expression analysis of planktonic and biofilm cultures +/- AZM were performed

using DEseq2 [70] (Supplementary Table S2). Genes with an adjusted P value (pAdj) < 0.1 were considered to have significant expression differences.

Detecting relative changes in intragenic transcription termination in the presence of AZM

Since transcription stalling or termination would result in reproducible peaks, we used reads corresponding to significant peaks of transcript ends in the intragenic (I) and 3'UTR regions (FL) of genes/operons for this analysis. Pseudocounts of 1 were used for all zero values from intragenic or full-length peaks. Cochran-Mantel-Haenszel tests were used to identify genes with significant differences between the expected and observed read frequencies in triplicate samples of untreated and treated cultures. The Benjamini-Hochberg procedure was used to control false discovery, with FDR < 0.1. Relative changes in levels of premature transcripts within the coding sequences of genes in response to AZM were estimated as the odds-ratio of intragenic / full length 3'-end peak read counts in AZM treated vs. untreated samples. Tests were performed in R (version 3.6.1) using default parameters in 2 x 2 x 3 matrices.

RESULTS

3pMap accurately identifies RNA 3'-OH ends

To investigate transcription-mediated regulatory mechanisms and the acute effects of AZM on the transcriptional landscape of *Pseudomonas aeruginosa,* we developed 3pMap. 3pMap adapts a commercially available RNA-seq kit to map mRNA 3'-ends, by ligating a custom 3'-end oligonucleotide adapter to total cellular RNA and directing library preparation to the adapter sequence (Figure 1A). Sequencing library synthesis using 3pMap has fewer steps compared to the Term-Seq approach [22] and requires minimal RNA input (2 µg) per sample.

We first applied 3pMap to *P. aeruginosa* PA14 grown under planktonic conditions in rich media in triplicate to evaluate its accuracy. We assessed the distribution of 3'-significant peaks in intragenic vs. intergenic regions of three classes of genes - tRNAs, protein coding sequences, and rRNAs (Supplementary Figure 2). Greater than 98% of significant peaks associated with tRNA genes were located within 3 nucleotides of the corresponding annotated 3'-ends (Supplementary Figure 2A-2B). Similarly, 99.8% of the significant peaks associated with 23S rRNAs mapped to their annotated 3'-ends (Supplementary Figure 2C-2D). Finally, 88.4% of significant peaks associated with mRNAs were located in intergenic

regions, with <12% located within coding sequences ((Supplementary Figure 2E). These results show that 3pMap accurately detects known RNA 3'-ends.

Interestingly, the majority of significant peaks associated with 5S rRNAs and 16S rRNAs were located -7/-8 (99.9%) and +35/+36 (80.54%) nucleotides, respectively, from their annotated 3'-ends (Supplementary Figure 2F-2H). The prokaryotic 5S rRNA sequence is well conserved and 120 nucleotides long, including in the PAO1 strain (Pseudomonas genome database). We aligned the 5S rRNA sequences from PAO1 and our PA14 using Clustal Omega (www.ebi.ac.uk), and found that the 3'-end identified by 3pMap is identical to PAO1 (Supplementary figure 2H). A recent study reported extended anti-Shine Dalgarno motifs in 16S rRNA in other bacteria, although they failed to identify such a motif in *P. aeruginosa* [71]. The major peak +35/36 downstream of 16S rRNA (Supplementary Figure 2F) could represent extended anti-Shine Dalgarno motifs in *P. aeruginosa* 16S rRNA, capable of providing additional specificity or transcript preference for Shine Dalgarno motifs on mRNA, or unprocessed pre-16S rRNAs [71,72]. Together, these results illustrate that 3pMap identifies both known and novel RNA 3' ends.

Predicting potential regulatory elements that cause transcription termination in *P. aeruginosa* transcript leaders

We next applied 3pMap to planktonic and biofilm cultures to predict novel genes regulated by early transcription termination. Transcription attenuators, riboswitches and RNA thermometers result in premature 3'-ends in the transcript leaders of bacterial genes [10-16]**.** We reasoned that transcript leaders regulated by early transcription termination would be characterized by a high incidence of 3'-end formation detectable by 3pMap. Therefore, we developed a computational pipeline to predict genes that are regulated by transcription termination in their early termination zone (transcript leader + 40 nucleotides in the coding sequence) (Figure 1B and Methods). We utilized the published transcript start sites from strain PAO1 [66] to define transcript leaders in PA14 by converting genome coordinates with liftOver [67]. We then calculated the percentage early termination (% ET) for each gene in planktonic and biofilm samples grown +/- AZM. The median %ET was < 3.0% for the tested samples (Figure 1B and Supplementary Figure 3B). A cut-off of 30%, which is >10-fold above the median %ET and sufficient to detect most riboswitches documented on Rfam (Supplementary Figure 3A and Supplementary Table S1), was used to predict outlier genes potentially regulated by early transcription termination. Genes with %ET values <30% and

lacking significant peaks representative of reproducible transcription pauses or stops in the transcript leaders were not considered in further analysis (Figure 2A).

We identified 282 protein-coding genes with more than 30% of their 3' ends in the early termination zone (Supplementary Table S2). These premature termination candidates include genes previously reported to be controlled by transcription termination in *P. aeruginosa*, such as the *amiE* operon (Figure 2B), *rhlA*, and *rhlI* (Supplementary Figure 3C) [73-75]. The gene with highest early transcription termination is *rhlI,* from whose transcript leader the sRNA *rhlS* was recently reported to be derived [76]. Genes known to be regulated by transcription attenuation in other bacteria, but not in *P. aeruginosa*, such as *pyrG* (Supplementary Figure 3D), *trpGCD* (Supplementary Figures 3E-3F), *rplJ*, and *lysR* family transcriptional regulators (PA14_68920 and PA14_71750) were also predicted to be regulated by early transcription termination [10,13,77,78]. Since attenuators, riboswitches, t-boxes, and RNA thermometers operate via formation of alternate structures that promote transcription termination or read-through, we examined the propensity for alternate structure formation upstream of the detected 3'-end peaks (predicted by PASIFIC) or Rho-independent termination sites (predicted by ARNold) [68,69] (Table 1). A number of premature termination candidate genes (41/282 early termination candidates), including *lasR* (Figure 2C), DNA gyrase A *gyrA* (Figure 2D), and the cytochrome c oxidase operon (not shown), were found to harbor putative riboregulator elements with a propensity to form alternate structures. The QS gene *lasR* regulates the expression of virulence factors in *P. aeruginosa* and therefore represents a particularly interesting therapeutic target [79]. Mutations of *gyrA* are common in fluroquinolone-resistant clinical strains [80] and inhibitors of *gyrA* expression are being explored as a pharmacological target [81,82]**.** In summary, 3pMap predicts regulation via transcriptional attenuation at hundreds of genes in *P. aeruginosa*, revealing potential new targets for molecular therapeutic intervention.

The effects of AZM on *P. aeruginosa* gene expression

We next investigated how AZM alters gene expression in *P. aeruginosa*, since bacterial transcription and translation are coupled [55-57]. To understand the acute response of *P. aeruginosa* to AZM, planktonic cultures were treated with the antibiotic for a short duration (20 minutes). Biofilm cultures were treated for a longer duration (3 hours) to account for barriers to drug penetration [29]. To assess gene expression changes in response to AZM, we performed differential expression analysis (DEseq2) using all reads from gene 3' UTR regions (Methods; Figure 1C, Figure 3A and Figure 3B, and Supplementary Table S3) with

an FDR of 10% (Supplementary Table S4). In AZM-treated planktonic cultures, 209 and 68 genes showed more than two-fold up- or down-regulation, respectively (Figure 3C). In biofilm cultures, 168 genes were downregulated and 112 genes were upregulated more than two-fold (Supplementary Table S4, Figure 3C). We observe little overlap between expression changes in planktonic and biofilm forms, potentially due to a combination of differences in duration of AZM treatment and lifestyle-specific gene expression patterns.

In AZM treated biofilms (Figure 3D), we observed reduced transcript levels of several global gene expression modulators associated with stress responses (*rpoS* [83,84]*, rpoH* [85], and *relA* [86])*,* anaerobic metabolism (*anr* [87,88])*,* virulence and biofilm formation (*rsmY* [89])*,* amino acid and nitrogen metabolism (*argR* [90]), *ntrBC* and *gdhB* [91]), QS (*vqsR* [92])*,* and antibiotic resistance *(amgR* [93]) (Figure 3D)*.* The expression of stress, virulence, biofilm, motility, and metabolism-related genes, many of which are controlled by these regulators, were also downregulated. In contrast, AZM treatment in biofilms upregulated expression of the *obgE* GTPase (also known as CgtA) more than 20-fold. Previous work suggests that ObgE is a key player in the stringent response and promotes bacterial persistence [61,94]. Overall, the functional categories in which multiple genes were differentially expressed here - inhibition of biofilm formation, AHL quorum sensing regulons, virulence, and stress responses - are broadly consistent with previously reported effects of AZM on *P. aeruginosa* [36,41,42,48]. However, our results better define several genetic pathways that may underlie these changes (Figure 3D).

In planktonic cells, AZM also downregulated the expression of global gene expression modulators *rpoS* [83,84]*, vqsR* [92]*,* and *algR* [95]*,* and promoted early transcription termination (Supplementary Table S6), but not significant downregulation, of *lasI*. As in biofilms, virulence factor genes were downregulated, though different genes were impacted (Figure 3E). These include phenazine biosynthesis genes *phzB2-G2* and *phzM* [96], *aprA* [97]*, lasB* (1.95-fold change in differential expression) *and rahU* [98]. Pilus genes *fimU* and *pilWXY1* were also downregulated, as were several heat shock proteins (*groEL, groES,* and *ibpA*, and *dnaK* [95, 99-101]). *mvfR (pqsR)*, a regulator of PQS quorum sensing [102], was upregulated, as was *obgE* though to a lesser extent than in biofilms (1.96-fold). In contrast to the biofilm samples, many genes associated with biofilm formation including *pelABCDEFG, gacA,* and the Wsp pathway were found to be upregulated upon AZM treatment, as well as haem biosynthesis proteins *hemL* and *hemE* [103-106]. The upregulation of biofilm genes is

in contrast to previous studies and potentially reflects the relatively shorter duration of AZM treatment we employed or other differences in growth conditions.

We leveraged 3pMap data to evaluate changes in the abundance of uncharged tRNA. Charged tRNA carry cognate amino-acids at their 3' ends, while uncharged tRNA have free 3'-OH ends. Thus, 3pMap detects uncharged tRNAs by 3'-adapter ligation to free 3'-OH ends during sequencing library synthesis. We observed significantly increased levels of uncharged tRNAs upon AZM treatment - one tRNA (tRNA-Val) in planktonic, and twelve tRNAs in biofilm samples (tRNA-Arg, tRNA-Gln, tRNA-Gly,and tRNA-Lys, tRNA-Pro, tRNA-Sec, tRNA-Thr, and tRNA-Val) (Supplementary Table S5). Interestingly, the tRNA isoacceptors detected here pair with rare codons in *P. aeruginosa* (Supplementary Table S5). In bacteria, translation and transcription elongation rates are affected by rare codons [107]. Translation efficiency is also positively correlated with tRNA levels [108]. Since bacterial transcription is co-translational [55-57,107], it is likely that increased levels of uncharged tRNAs that pair with certain rare codons impacts the transcription of genes enriched for codons that pair with them in *P. aeruginosa*. Additionally, uncharged tRNAs induce stringent response, which in turn promotes bacterial persistence [109], and regulate target genes containing t-box domains [15].

A major role for premature transcription termination in *P. aeruginosa* response to AZM

Previous work reported chronic AZM treatment impairs biofilm formation by inhibiting the expression of the *lasI/lasR* and *rhlI/rhlR* QS systems [39,42,43]. QS inhibition is proposed to be achieved via downregulation of the *las* and *rhl* genes [39], or downregulation of enzymes responsible for QS effector synthesis [43]. The molecular mechanisms underlying AZM-mediated regulation of QS regulators have not been determined. Although *lasI, lasR, rhlI,* and *rhlR* were not significantly downregulated in our results, we observed significant premature transcription termination or pausing peaks in *lasI* and *rhlR* upon AZM treatment (Figures 4A and Figure 4B). We used the ratio of reads at intragenic peaks to full length peaks in 3' UTRs (I/FL) as a metric for premature transcription termination and evaluated relative differences in I/FL in AZM-treated and untreated samples using CMH tests with a 10% FDR (Methods and Figure 1C). AZM-treatment led to altered I/FL in 668 (23.5%) and 389 (13.7%) genes in biofilm and planktonic cultures, respectively (Table S6). Notably, AZM treatment resulted in extensive premature termination in the 5'-end of *lasI* and a

correspondingly large increase in I/FL in biofilms (~41-fold) and in planktonic cultures (~16-fold) (Figure 4A). Similarly, an ~8-fold increase in I/FL was also observed in the *rhlR* gene in AZM treated biofilms (Figure 4B). Our results show that AZM disrupts full length *lasI* and *rhlR* expression by inducing premature transcription termination or pausing within their coding sequences.

We next investigated whether the changes in premature transcript levels were a pervasive feature of protein-coding genes differentially regulated by AZM (Figure 1C and Supplementary Table S6). In biofilms, 256 differentially expressed genes had I/FL ratio measurements, and 134 of these changed significantly with AZM treatment. In planktonic cultures, I/FL measurements were available for 290 differentially expressed genes, and 89 changed with AZM treatment. Thus, differentially expressed genes were enriched ~ 2.2-fold for changes in I/FL in both biofilm and planktonic culture. Notably, two thirds (115 of 169) of genes downregulated by AZM in biofilms had increased levels of premature transcripts compared to full length transcripts (e.g. Figure 4C and 4D). These include well-known *P. aeruginosa* regulators *rpoS, anr*, and *relA,* as well as genes involved in biofilm formation, stress response, and virulence factor genes such as *hemN* (Figure 4C), *lasB* (Figure 4D), *rahU, phzB1-G1* and *pelABCDEFG* [83,84,86,87,98,110]. The targets that exhibit no evidence of early transcription termination in their transcript leaders, yet are still significantly downregulated upon AZM treatment, may reflect expression changes in upstream regulators by AZM. The *lecB*, *argR*, and *sodB* genes are notable examples [42,49,90,111].

Changes in premature transcription termination could also reciprocally contribute to upregulation of genes in response to AZM treatment. Indeed, 19 of the 87 upregulated genes in biofilms, and 75 of the 212 genes upregulated in planktonic cultures exhibited corresponding decreases in premature transcription termination. The most upregulated gene in AZM-treated biofilms is *obgE*, a conserved GTPase involved in the stringent response and persistence in *P. aeruginosa* [61,94]. Notably, *obgE* also showed the highest reduction in I/FL peak ratio in response to AZM through a striking reduction in premature transcription termination at the ObgE start codon (Figure 3E and Figure 3F). Thus, relief of premature transcription termination occurs at most genes upregulated by AZM and may contribute to induction of the stringent response.

DISCUSSION

In this study, we used 3pMap to identify RNA 3'-ends in *P. aeruginosa* and to gain insights into gene regulation in response to AZM. We identified over two hundred genes exhibiting high levels of premature transcription termination in their transcript leaders. Dozens of these genes are predicted to form alternate structures in their transcript leaders, and hence could be controlled by riboswitches and attenuators (Table 1). In addition, our study provides new insights into the role of transcriptional regulation in the *P. aeruginosa* response to AZM. Most downregulated genes, including many key transcriptional regulators and their targets - exhibit enhanced premature transcription termination that contributes to the suppressive effects of AZM on QS and virulence factor transcription. We also found reduced transcription attenuation in some upregulated genes upon AZM treatment, most notably inducing expression of *obgE*, a central component of the stringent response. The implications of these results for understanding *P. aeruginosa* biology and therapeutic interventions are discussed below.

RNA-based regulatory strategies are gaining traction as antibacterial therapeutic targets [17,112-114]. For example, the FMN riboswitch controls expression of flavin mononucleotide synthesis operons in many bacteria. Ribocil, a small molecule that targets the riboswitch by mimicking the FMN ligand, reduced bacterial growth of *E. coli* in a mouse systemic infection model [112]**.** Similarly, a small molecule targeting the guanine riboswitch, PC1, inhibited growth of *S. aureus* in mouse and cow infection models [114,115]. The candidate riboregulators we identified provide a first transcriptome-wide catalogue of potentially "druggable RNAs" in *P. aeruginosa*. However, due to the compact nature of bacterial genomes, some of the candidate riboregulators may represent termination sites from upstream genes. On the other hand, many riboswitches and attenuators may still await discovery, as these elements are condition-specific and may require interactions with the host immune system or other cellular stresses for their activity. Thus, further studies are needed to identify the full set of bonafide riboregulators in *P. aeruginosa* and determine their molecular mechanisms and feasibility as drug targets.

Chronic *P. aeruginosa* infections are common in CF patients, and sub-inhibitory concentrations of AZM improve clinical outcomes [31,32,24]. AZM impairs biofilm formation due to altered expression of QS and virulence genes [39-46,48]. Previous work proposed the effects of AZM on QS resulted from inhibition of the synthesis of specific proteins [39,43]. First, AZM might disrupt the translation of an unknown protein which in turn controls the transcription of autoinducer synthases *lasI and rhlI* [39]. Secondly, AZM might

downregulate the expression of N-acyl homoserine lactone (AHL) synthesis enzymes upstream of *lasI* and *rhlI*, which in turn further dampen AHL production and inhibit QS [43]. However, because the assays used in these previous studies did not differentiate between full-length and truncated transcripts, neither of the resulting models consider the impact of AZM-induced translational stalling on coupled mRNA transcription. We investigated the role of transcription termination on the *P. aeruginosa* response to AZM using 3pMap. AZM greatly elevated the levels of premature transcripts in primary QS regulators *lasI* (in planktonic and biofilm cultures) and *rhlR* (in biofilms) (Figure 4A and Figure 4B). Thus, our results suggest AZM directly impacts expression of QS genes by inducing premature transcription termination.

Importantly, we found AZM also induced premature transcripts in key transcriptional regulators of biofilm formation and virulence (Supplementary Table S6). Such increases in premature transcript formation accompanied the downregulation of *rpoS, rpoH, vqsR* and *anr* [83-85,87,88,92]. *Anr* regulates QS and virulence gene expression in low-oxygen environments such as biofilms [87,88]. In QS mutants isolated from infections, *anr* plays a compensatory role in virulence gene expression. The expression of *rpoS*, an alternative sigma factor and a master regulator of *P. aeruginosa* stress response [83,84] was downregulated by AZM in planktonic cells as well. Increased premature transcription termination also accompanied downregulation of virulence factors genes targeted by QS (*lasB, phzB-G, pelABCD, rahU*) [42,96-98,116]. Taken together, our results support a model in which AZM-induced premature transcription termination reduces the expression of these central transcriptional modulators (Fig 5A), with corresponding decreases in the expression of their downstream targets, and at times direct regulation of these targets as well (Figure 5B).

The effects of AZM on *P. aeruginosa* gene expression are reminiscent of previous work in other bacteria, which showed ribosome-acting antibiotics can alter target gene transcription by stalling translation [55,107,117-119]. In *E.coli,* slowing translation with sublethal concentrations of chloramphenicol uncouples transcription from translation, thereby slowing transcription elongation rates and/or triggering premature transcription termination [107,119]**.** Macrolide-mediated ribosome stalling is not uniformly distributed across genes but instead is determined by specific sequence features of nascent polypeptides [120]. In *Staphylococcus aureus*, AZM caused sequence-specific ribosome stalling in the middle or late stages of translation [51,52]. Interestingly, AZM-specific ribosome stalling hotspots,

referred to as ‘macrolide arrest motifs’ [121], were enriched in virulence-related and essential genes [120]. By quantifying premature transcription, we found premature transcription termination, most likely due to AZM-induced ribosome stalling, occurs at most, if not all, downregulated genes in *P. aeruginosa*. The enhanced premature transcription termination in *P. aeruginosa* genes likely reflects such sequence-specific ribosome stalling. One interesting possibility is that *P. aeruginosa* has evolved macrolide-responsive stall sequences in QS and stress response genes (e.g. *rpoS* and *lasI*) to promote survival in response to macrolides produced by environmental competitors [122]. Additional studies, including ribosome profiling, are needed to identify translation stalling motifs in *P. aeruginosa* and further investigate antibiotic induced ribosome stalling on transcription.

We further utilized 3pmap data to evaluate changes in tRNA charging in response to AZM. The increased levels of uncharged rare-codon tRNAs in AZM treated cells could further disrupt translation, and thereby transcription [117,118]. The influence of rare codons on translation and transcription elongation rates is well documented in *E. coli* [107], and tRNA concentrations and codon decoding times are positively correlated in many prokaryotes [108,117]. Interestingly, replacing a rare codon (AGG, frequency = 0.6 / 1000) for Arginine at the second codon position of the QS gene *rhlR* with the most frequently used codon (CGC, frequency = 48.8 / 1000) was previously shown to alleviate the inhibitory effects of AZM on virulence factor production in *P. aeruginosa* [123]**.** Our results suggest tRNAs targeting rare codons for Arg, Lys, Pro, Gln, Gly, Sec, and Val were more often uncharged after AZM treatment in biofilms. This decrease in tRNA charging could cause ribosome stalling at rare codons, altering the synthesis of full-length transcripts (Figure 5). Whether the elevated levels of uncharged tRNAs observed in this study result from ribosome stalling on specific sequences, recycling of peptidyl-tRNAs, or other mechanisms remains to be determined.

We also found that AZM treatment caused upregulation of *obgE*, a conserved GTPase that binds ppGpp and mediates the bacterial stringent response and persistence (Figures 4E and 4F) [94, 61]. On binding to guanosine tetraphosphate (ppGpp), the global stringent response alarmone, ObgE facilitates increased dissociation of 70S ribosomal subunits [124] **.** An interesting possibility is that ObgE facilitates the release of ribosomes stalled by AZM. 3pMap identified prominent premature transcription in the first codon of the *obgE* ORF. AZM-induced upregulation of *obgE* coincided with reduced levels of premature transcription termination, suggesting it may be regulated by a transcriptional attenuator.

Although uncharged tRNA levels were elevated (Supplementary Table S4), the *relA* gene [86], which produces the central stringent response alarmone (p)ppGpp, was notably downregulated. The function of *obgE* in promoting bacterial persistence is thought to require (p)ppGpp [61], therefore while its overexpression may promote persistence, other components of the stringent response may actually be downregulated, and it is unclear if this impedes the effect of overexpression of *obgE*.

Transcription attenuators control termination through the formation of alternative RNA structures in response to small molecules, uncharged tRNA (T-boxes), interactions with RNA binding proteins, and ribosome stalling in short upstream open reading frames (uORFs) [10,11,15,16]**.** Recent work found ribosome stalling on uORFs relieved premature transcription termination of antibiotic resistance genes in response to the macrolide lincomycin, promoting full length transcription in *L. monocytogenes* and other bacteria [22]. Curiously, the *obgE* transcript leader contains a uORF (Figure 4F), which may play a similar role in upregulating full-length transcription through attenuation. However, this attenuation-by-uORF mechanism seems insufficient because the observed premature termination occurs at the *obgE* start codon, which is followed by a rare codon for lysine, not in an intrinsic terminator. This suggests additional regulatory factors may contribute to the switch to full length transcription in the presence of azithromycin. For example, the switch to full length transcription may be independent of the uORF, instead relying on *rho,* other *trans*-acting factors or uncharged tRNA. Future work is needed to resolve these possibilities.

Regardless of the molecular mechanisms utilized, our results suggest that premature transcription termination plays a key role in the response to AZM by *P. aeruginosa* by regulating QS and virulence gene expression. We propose a model in which the AZM-induced premature termination of central transcriptional modulators cascades through their regulatory targets (Figure 5). Furthermore, the AZM-dependent increases in uncharged tRNAs and induced *obgE* expression we observed suggest that AZM triggers the stringent response and persistence in *P. aeruginosa*. This implies that the efficacy of AZM as an anti-virulence treatment may trade off against the induction of persister phenotypes, a phenomenon warranting further study. In summary, the candidate riboregulators we identified provide both new potential therapeutic targets, and we provide new insights into how AZM treatment affects *Pseudomonas* biofilms, which may contribute to improved treatments for chronic persistent *P. aeruginosa* infections.

ACKNOWLEDGEMENTS

This work was supported by the National Institute of General Medical Sciences (grant R01GM121895) to C.J.M. and by the National Institute of Allergy and Infectious Diseases at the National Institutes of Health (grant U01AI124302 and grant T32AI049820) and by the Cystic Fibrosis Foundation Research Development Program to V.S.C.

DATA AVAILABILITY

High-throughput sequencing data have been submitted to NCBI under Bioproject accession number PRJNA639207 and will be released upon publication.

REFERENCES

1. Peleg AY, Hooper DC. Hospital-acquired infections due to gram-negative bacteria. N Engl J Med. 2010;362: 1804–1813. doi:10.1056/NEJMra0904124
2. Driscoll JA, Brody SL, Kollef MH. The epidemiology, pathogenesis and treatment of *Pseudomonas aeruginosa* infections. Drugs. 2007;67: 351–368. doi:10.2165/00003495-200767030-00003
3. Gellatly SL, Hancock RE. *Pseudomonas aeruginosa:* new insights into pathogenesis and host defenses. Pathogens Disease. 2013;67: 159–173. doi:10.1111/2049-632X.12033
4. Ramirez Estrada, S., Borgatta, B., & Rello, J. *Pseudomonas aeruginosa* ventilator-associated pneumonia management. Infection and Drug Resistance. 2015;9: 7–18. http://doi.org/10.2147/IDR.S50669
5. Wu DC, Chan WW, Metelitsa AI, Fiorillo L, Lin AN. Pseudomonas skin infection: clinical features, epidemiology, and management. Am J Clin Dermatol. 2011;12: 157–169. doi:10.2165/11539770-000000000-00000
6. Lister PD, Wolter DJ, Hanson ND. Antibacterial-resistant *Pseudomonas aeruginosa*: Clinical impact and complex regulation of chromosomally encoded resistance mechanisms. Clinical Microbiology Reviews. 2009;22: 582–610. doi:10.1128/CMR.00040-09
7. Cattaneo C, Casari S, Bracchi F, Signorini L, Ravizzola G, Borlenghi E, et al. Recent increase in enterococci, viridans streptococci, Pseudomonas spp. and multiresistant strains among haematological patients, with a negative impact on outcome. Results of a 3-year surveillance study at a single institution. Scand J Infect Dis. 2010;42: 324–332. doi:10.3109/00365540903496569
8. Tacconelli E, Carrara E, Savoldi A, Harbarth S, Mendelson M, Monnet DL, et al. Discovery, research, and development of new antibiotics: the WHO priority list of antibiotic-resistant bacteria and tuberculosis. The Lancet Infectious Diseases. 2018;18: 318–327. doi:10.1016/S1473-3099(17)30753-3

9. Breidenstein EBM, la Fuente-Núñez de C, Hancock REW. *Pseudomonas aeruginosa*: all roads lead to resistance. Trends in Microbiology. 2011;19: 419–426. doi:10.1016/j.tim.2011.04.005
10. Henkin TM, Yanofsky C. Regulation by transcription attenuation in bacteria: how RNA provides instructions for transcription termination/antitermination decisions. Bioessays. 2002;24: 700–707. doi:10.1002/bies.10125
11. Merino E, Yanofsky C. Transcription attenuation: a highly conserved regulatory strategy used by bacteria. Trends in Genetics. 2005;21: 260–264. doi:10.1016/j.tig.2005.03.002
12. Abduljalil JM. Bacterial riboswitches and RNA thermometers: Nature and contributions to pathogenesis. Noncoding RNA Res. 2018;3: 54–63. doi:10.1016/j.ncrna.2018.04.003
13. Naville M, Gautheret D. Transcription attenuation in bacteria: theme and variations. Brief Funct Genomic Proteomic. 2009;8: 482–492. doi:10.1093/bfgp/elp025
14. Kortmann J, Narberhaus F. Bacterial RNA thermometers: molecular zippers and switches. Nat Rev Microbiol. 2012;10: 255–265. doi:10.1038/nrmicro2730
15. Green NJ., Grundy FJ, & Henkin TM The T box mechanism: tRNA as a regulatory molecule. FEBS Letters. 2010;584: 318–324. doi:10.1016/j.febslet.2009.11.056
16. Winkler WC, Breaker RR. Regulation of bacterial gene expression by riboswitches. Annu Rev Microbiol. 2005;59: 487–517. doi:10.1146/annurev.micro.59.030804.121336
17. Disney MD, Dwyer BG, Childs-Disney JL. Drugging the RNA World. Cold Spring Harb Perspect Biol 2018;10: a034769. doi:10.1101/cshperspect.a034769
18. Nshogozabahizi JC, Aubrey KL, Ross JA, Thakor N. Applications and limitations of regulatory RNA elements in synthetic biology and biotechnology. Journal of Applied Microbiology. 2019;127: 968–984. doi:10.1111/jam.14270
19. Etzel M, Mörl M. Synthetic riboswitches: From plug and pray toward plug and play. Biochemistry. 2017;56: 1181–1198. doi:10.1021/acs.biochem.6b01218
20. Borges A, Simões M, Todorović TR, Filipović NR, García-Sosa AT. Cobalt complex with thiazole-based ligand as new *Pseudomonas aeruginosa* quorum quencher. biofilm inhibitor and virulence attenuator. 2018;23: 1385. doi:10.3390/molecules23061385
21. Johansson J, Mandin P, Renzoni A, Chiaruttini C, Springer M, Cossart P. An RNA thermosensor controls expression of virulence genes in *Listeria monocytogenes*. Cell. 2002;110: 551–561. doi:10.1016/s0092-8674(02)00905-4

22. Dar D, Shamir M, Mellin JR, Koutero M, Stern-Ginossar N, Cossart P, Sorek R. Term-seq reveals abundant ribo-regulation of antibiotics resistance in bacteria. Science. 2016;352: aad9822–aad9822. doi:10.1126/science.aad9822
23. Irnov I, Winkler WC. A regulatory RNA required for antitermination of biofilm and capsular polysaccharide operons in Bacillales. Molecular Microbiology. 2010;76: 559–575. doi:10.1111/j.1365-2958.2010.07131.x
24. Warrier I, Ram-Mohan N, Zhu Z, Hazery A, Echlin H, Rosch J, Meyer MM, van Opinjen T. The Transcriptional landscape of *Streptococcus pneumoniae* TIGR4 reveals a complex operon architecture and abundant riboregulation critical for growth and virulence. PLoS Pathog. 2018;14: e1007461. doi:10.1371/journal.ppat.1007461
25. Flemming H-C, Wingender J, Szewzyk U, Steinberg P, Rice SA, Kjelleberg S. Biofilms: an emergent form of bacterial life. Nat Rev Microbiol. 2016;14: 563–575. doi:10.1038/nrmicro.2016.94
26. Wei, Q, Ma LZ. Biofilm matrix and its regulation in *Pseudomonas aeruginosa*. International Journal of Molecular Sciences. 2013;14: 20983–21005. http://doi.org/10.3390/ijms141020983
27. Jolivet-Gougeon A, Bonnaure-Mallet M. Biofilms as a mechanism of bacterial resistance. Drug Discov Today Technol. 2014;11: 49–56. doi:10.1016/j.ddtec.2014.02.003
28. Bjarnsholt T. The role of bacterial biofilms in chronic infections. APMIS. Supplementum; 2013;: 1–51. doi:10.1111/apm.12099
29. Mulcahy LR, Isabella VM, Lewis K. *Pseudomonas aeruginosa* biofilms in disease. Microb Ecol. 2014;68: 1–12. doi:10.1007/s00248-013-0297-x
30. Høiby N, Krogh Johansen H, Moser C, Song Z, Ciofu O, Kharazmi A. *Pseudomonas aeruginosa* and the *in vitro* and *in vivo* biofilm mode of growth. Microbes Infect. 2001;3: 23–35. doi:10.1016/s1286-4579(00)01349-6
31. Howe RA, Spencer RC. Macrolides for the treatment of *Pseudomonas aeruginosa* infections? J Antimicrob Chemother. 1997;40: 153–155. doi:10.1093/jac/40.2.153
32. Schultz MJ. Macrolide activities beyond their antimicrobial effects: macrolides in diffuse panbronchiolitis and cystic fibrosis. J Antimicrob Chemother. 2004;54: 21–28. doi:10.1093/jac/dkh309
33. Blasi F, Bonardi D, Aliberti S, Tarsia P, Confalonieri M, Amir O, Carone M, Marco FD, Centanni S, Guffanti E. Long-term azithromycin use in patients with chronic

obstructive pulmonary disease and tracheostomy. Pulm Pharmacol Ther. 2010;23: 200–207. doi:10.1016/j.pupt.2009.12.002

34. Yousef AA, Jaffe A. The role of azithromycin in patients with cystic fibrosis. Paediatr Respir Rev. 2010;11: 108–114. doi:10.1016/j.prrv.2009.12.003
35. Taylor SP, Sellers E, Taylor BT. Azithromycin for the Prevention of COPD Exacerbations: The Good, Bad, and Ugly. Am J Med. 2015;128: 1362.e1–6. doi:10.1016/j.amjmed.2015.07.032
36. Hoffmann N, Lee B, Hentzer M, Rasmussen TB, Song Z, Johansen HK, Givskov M, Høiby N. Azithromycin blocks quorum sensing and alginate polymer formation and increases the sensitivity to serum and stationary-growth-phase killing of *Pseudomonas aeruginosa* and attenuates chronic *P. aeruginosa* lung infection in Cftr(-/-) mice. Antimicrob Agents Chemother. 2007;51: 3677–3687. doi:10.1128/AAC.01011-06
37. Stellari F, Bergamini G, Sandri A, Donofrio G, Sorio C, Ruscitti F, Villetti G, Assael BM, Melotti P, Lleo MM. In vivo imaging of the lung inflammatory response to *Pseudomonas aeruginosa* and its modulation by azithromycin. J Transl Med. 2015;13: 251–10. doi:10.1186/s12967-015-0615-9
38. Davies DG, Parsek MR, Pearson JP, Iglewski BH, Costerton JW, Greenberg EP. The involvement of cell-to-cell signals in the development of a bacterial biofilm. Science. 1998;280: 295–298. doi:10.1126/science.280.5361.295
39. Tateda K, Comte R, Pechere JC, Köhler T, Yamaguchi K, Van Delden C. Azithromycin inhibits quorum sensing in *Pseudomonas aeruginosa*. Antimicrob Agents Chemother. 2001;45: 1930–1933. doi:10.1128/AAC.45.6.1930-1933.2001
40. Favre-Bonté S, Köhler T, Van Delden C. Biofilm formation by *Pseudomonas aeruginosa*: role of the C4-HSL cell-to-cell signal and inhibition by azithromycin. J Antimicrob Chemother. 2003;52: 598–604. doi:10.1093/jac/dkg397
41. Gillis RJ, Iglewski BH. Azithromycin retards *Pseudomonas aeruginosa* biofilm formation. Journal of Clinical Microbiology. American Society for Microbiology Journals; 2004;42: 5842–5845. doi:10.1128/JCM.42.12.5842-5845.2004
42. Nalca Y, Jänsch L, Bredenbruch F, Geffers R, Buer J, Häussler S. Quorum-sensing antagonistic activities of azithromycin in *Pseudomonas aeruginosa* PAO1: a global approach. Antimicrob Agents Chemother. 2006;50: 1680–1688. doi:10.1128/AAC.50.5.1680-1688.2006
43. Kai T, Tateda K, Kimura S, Ishii Y, Ito H, Yoshida H, Kimura T, Yamaguchi K. A low concentration of azithromycin inhibits the mRNA expression of N-acyl homoserine

lactone synthesis enzymes, upstream of lasI or rhlI, in *Pseudomonas aeruginosa*. Pulm Pharmacol Ther. 2009;22: 483–486. doi:10.1016/j.pupt.2009.04.004

44. Skindersoe ME, Alhede M, Phipps R, Yang L, Jensen PO, Rasmussen TB, Bjarnsholt T, Tolker-Nielsen T, Høiby N, Givskov M. Effects of antibiotics on quorum sensing in *Pseudomonas aeruginosa*. Antimicrob Agents Chemother. 2008;52: 3648–3663. doi:10.1128/AAC.01230-07
45. Swatton JE, Davenport PW, Maunders EA, Griffin JL, Lilley KS, Welch M. Impact of azithromycin on the quorum sensing-controlled proteome of *Pseudomonas aeruginosa*. PLoS ONE. 2016;11: e0147698. doi:10.1371/journal.pone.0147698
46. Molinari G, Guzmán CA, Pesce A, Schito GC. Inhibition of *Pseudomonas aeruginosa* virulence factors by subinhibitory concentrations of azithromycin and other macrolide antibiotics. J Antimicrob Chemother. 1993;31: 681–688. doi:10.1093/jac/31.5.681
47. Molinari G, Paglia P, Schito GC. Inhibition of motility of *Pseudomonas aeruginosa* and *Proteus mirabilis* by subinhibitory concentrations of azithromycin. Eur J Clin Microbiol Infect Dis. 1992;11: 469–471. doi:10.1007/bf01961867
48. Imperi F, Leoni L, Visca P. Antivirulence activity of azithromycin in *Pseudomonas aeruginosa*. Front Microbiol. Frontiers; 2014;5: 10. doi:10.3389/fmicb.2014.00178
49. Hassett DJ, Ma JF, Elkins JG, McDermott TR, Ochsner UA, West SE, et al. Quorum sensing in *Pseudomonas aeruginosa* controls expression of catalase and superoxide dismutase genes and mediates biofilm susceptibility to hydrogen peroxide. Molecular Microbiology. 1999;34: 1082–1093. doi:10.1046/j.1365-2958.1999.01672.x
50. Retsema J, Girard A, Schelkly W, Manousos M, Anderson M, Bright G, et al. Spectrum and mode of action of azithromycin (CP-62,993), a new 15-membered-ring macrolide with improved potency against gram-negative organisms. Antimicrob Agents Chemother. 1987;31: 1939–1947. doi:10.1128/aac.31.12.1939
51. Kannan K, Vázquez-Laslop N, & Mankin AS. Selective protein synthesis by ribosomes with a drug-obstructed exit tunnel. Cell. 2012;151: 508–520. http://doi.org/10.1016/j.cell.2012.09.018
52. Kannan K, Mankin AS. Macrolide antibiotics in the ribosome exit tunnel: species-specific binding and action. Ann N Y Acad Sci. 2011;1241: 33–47. doi:10.1111/j.1749-6632.2011.06315.x
53. Hansen JL, Ippolito JA, Ban N, Nissen P, Moore PB, Steitz TA. The structures of four macrolide antibiotics bound to the large ribosomal subunit. Molecular Cell. 2002;10: 117–128. doi:10.1016/S1097-2765(02)00570-1

54. Sothiselvam S, Liu B, Han W, Ramu H, Klepacki D, Atkinson GC, et al. Macrolide antibiotics allosterically predispose the ribosome for translation arrest. PNAS. 2014;111: 9804–9809. doi:10.1073/pnas.1403586111
55. McGary K, Nudler E. RNA polymerase and the ribosome: the close relationship. Curr Opin Microbiol. 2013;16: 112–117. doi:10.1016/j.mib.2013.01.010
56. Fan H, Conn AB, Williams PB, Diggs S, Hahm J, Gamper HB, Hou YM, O'Leary SE, Wang Y, Blaha GM. Transcription-translation coupling: direct interactions of RNA polymerase with ribosomes and ribosomal subunits. Nucleic Acids Research. 2017;45: 11043–11055. doi:10.1093/nar/gkx719
57. Conn AB, Diggs S, Tam TK, Blaha GM. Two old dogs, one new trick: A review of RNA polymerase and ribosome interactions during transcription-translation coupling. International Journal of Molecular Sciences. 2019;20: 2595. doi:10.3390/ijms20102595
58. Tandonnet S, Torres TT. Traditional versus 3′ RNA-seq in a non-model species. Genomics Data. 2017;11: 9–16. doi:10.1016/j.gdata.2016.11.002
59. Ma F, Fuqua BK, Hasin Y, Yukhtman C, Vulpe CD, Lusis AJ, Pellegrini M. A comparison between whole transcript and 3' RNA sequencing methods using Kapa and Lexogen library preparation methods. BMC Genomics. 2019;20: 9. doi:10.1186/s12864-018-5393-3
60. Corley SM, Troy NM, Bosco A, Wilkins MR. QuantSeq 3′ sequencing combined with Salmon provides a fast, reliable approach for high throughput RNA expression analysis. Sci Rep. 2019;9: 1–15. doi:10.1038/s41598-019-55434-x
61. Verstraeten N, Knapen WJ, Kint CI, Liebens V, Van den Bergh B, Dewachter L, et al. Obg andmembrane depolarization are part of a microbial bet-hedging strategy that leads to antibiotic tolerance. Molecular Cell. Cell Press; 2015;59: 9–21. doi:10.1016/j.molcel.2015.05.011
62. Martin M. Cutadapt removes adapter sequences from high-throughput sequencing reads. EMBnetjournal. 2011;17: 10–12. doi:10.14806/ej.17.1.200
63. Ben Langmead, Salzberg SL. Fast gapped-read alignment with Bowtie 2. Nat Methods. 2012;9: 357–359. doi:10.1038/nmeth.1923
64. Quinlan AR, Hall IM. BEDTools: a flexible suite of utilities for comparing genomic features. Bioinformatics. 2010;26: 841–842. doi:10.1093/bioinformatics/btq033

65. Freese NH, Norris DC, Loraine AE. Integrated genome browser: visual analytics platform for genomics. Bioinformatics. 2016;32: 2089–2095. doi:10.1093/bioinformatics/btw069
66. Wurtzel O, Yoder-Himes DR, Han K, Dandekar AA, Edelheit S, Greenberg EP, Sorek R, Lory S. The single-nucleotide resolution transcriptome of *Pseudomonas aeruginosa* grown in body temperature. PLoS Pathog. 2012;8: e1002945. doi:10.1371/journal.ppat.1002945
67. Kent WJ, Sugnet CW, Furey TS, Roskin KM, Pringle TH, Zahler AM, et al. The human genome browser at UCSC. Genome Res. 2002;12: 996–1006. doi:10.1101/gr.229102
68. Millman A, Dar D, Shamir M, Sorek R. Computational prediction of regulatory, premature transcription termination in bacteria. Nucleic Acids Research. 2017;45: 886–893. doi:10.1093/nar/gkw749
69. Naville M, Ghuillot-Gaudeffroy A, Marchais A, Gautheret D. ARNold: a web tool for the prediction of Rho-independent transcription terminators. RNA Biol. 2011;8: 11–13. doi:10.4161/rna.8.1.13346
70. Love MI, Huber W, Anders S. Moderated estimation of fold change and dispersion for RNA-seq data with DESeq2. Genome Biol. 2014;15: 1–21. doi:10.1186/s13059-014-0550-8
71. Silke JR, Wei Y, Xia X. RNA-Seq-based analysis reveals heterogeneity in mature 16S rRNA 3' termini and extended anti-Shine-Dalgarno motifs in bacterial species. G3: Genes, Genomes, Genetics; 2018;8: 3973–3979. doi:10.1534/g3.118.200729
72. Kaczanowska M, Rydén-Aulin M. Ribosome biogenesis and the translation process in *Escherichia coli*. Microbiol Mol Biol Rev. 2007;71: 477–494. doi:10.1128/MMBR.00013-07
73. Wilson SA, Wachira SJ, Norman RA, Pearl LH, Drew RE. Transcription antitermination regulation of the *Pseudomonas aeruginosa* amidase operon. The EMBO Journal. 1996;15: 5907–5916. doi:10.1002/j.1460-2075.1996.tb00977.x
74. Grosso-Becerra MV, Croda-García G, Merino E, Servín-González L, Mojica-Espinosa R, Soberón-Chávez G. Regulation of *Pseudomonas aeruginosa* virulence factors by two novel RNA thermometers. Proc Natl Acad Sci USA. 2014;111: 15562–15567. doi:10.1073/pnas.1402536111
75. Ochsner UA, Reiser J. Autoinducer-mediated regulation of rhamnolipid biosurfactant synthesis in *Pseudomonas aeruginosa*. PNAS. 1995;92: 6424–6428. doi:10.1073/pnas.92.14.6424

76. Thomason MK, Voichek M, Dar D, Addis V, Fitzgerald D, Gottesman S, Sorek R, Greenberg E. A rhlI 5′ UTR-derived sRNA regulates RhlR-dependent quorum sensing in *Pseudomonas aeruginosa*. mBio. 2019;10: 43. doi:10.1128/mBio.02253-19
77. Turnbough CL, Switzer RL. Regulation of pyrimidine biosynthetic gene expression in bacteria: Repression without repressors. Microbiol Mol Biol Rev. 2008;72: 266.
78. Du H, Tarpey R, Babitzke P. The *trp* RNA-binding attenuation protein regulates TrpG synthesis by binding to the *trpG* ribosome binding site of *Bacillus subtilis*. J Bacteriol. 1997;179: 2582–2586. doi:10.1128/jb.179.8.2582-2586.1997
79. Gilbert KB, Kim TH, Gupta R, Greenberg EP, Schuster M. Global position analysis of the *Pseudomonas aeruginosa* quorum-sensing transcription factor LasR. Molecular Microbiology. 2009;73: 1072–1085. doi:10.1111/j.1365-2958.2009.06832.x
80. Mouneimné H, Robert J, Jarlier V, Cambau E. Type II topoisomerase mutations in ciprofloxacin-resistant strains of *Pseudomonas aeruginosa*. Antimicrob Agents Chemother. 1999;43: 62–66.
81. Kaguni JM. The macromolecular machines that duplicate the *Escherichia coli* chromosome as targets for drug discovery. Antibiotics. 2018;7: 23. doi:10.3390/antibiotics7010023
82. Dages S, Dages K, Zhi X, Leng F. Inhibition of the *gyrA* promoter by transcription-coupled DNA supercoiling in *Escherichia coli*. Sci Rep. 2018;8: 1–9. doi:10.1038/s41598-018-33089-4
83. Whiteley M, Parsek MR, Greenberg EP. Regulation of quorum sensing by RpoS in *Pseudomonas aeruginosa*. J Bacteriol. 2000;182: 4356–4360. doi:10.1128/JB.182.15.4356-4360.2000
84. Schuster M, Hawkins AC, Harwood CS, Greenberg EP. The *Pseudomonas aeruginosa* RpoS regulon and its relationship to quorum sensing. Molecular Microbiology. 2004;51: 973–985. doi:10.1046/j.1365-2958.2003.03886.x
85. Potvin E, Sanschagrin F, Levesque RC. Sigma factors in *Pseudomonas aeruginosa*. FEMS Microbiol Rev. 2008;32: 38–55. doi:10.1111/j.1574-6976.2007.00092.x
86. Erickson DL, Lines JL, Pesci EC, Venturi V, Storey DG. *Pseudomonas aeruginosa relA* contributes to virulence in *Drosophila melanogaster.* Infect Immun. 2004;72: 5638–5645. doi:10.1128/IAI.72.10.5638-5645.2004
87. Rompf A, Hungerer C, Hoffmann T, Lindenmeyer M, Römling U, Groß U, Doss MO, Arai H, Igarashi Y, Jahn D. Regulation of *Pseudomonas aeruginosa hemF* and *hemN*

by the dual action of the redox response regulators Anr and Dnr. Molecular Microbiology. 1998;29: 985–997. doi:10.1046/j.1365-2958.1998.00980.x

88. Hammond JH, Dolben EF, Smith TJ, Bhuju S, Hogan DA. Links between Anr and Quorum Sensing in *Pseudomonas aeruginosa* biofilms. J Bacteriol. 2015;197: 2810–2820. doi:10.1128/JB.00182-15
89. Pérez-Martínez I, Haas D. Azithromycin inhibits expression of the GacA-dependent small RNAs RsmY and RsmZ in *Pseudomonas aeruginosa.* Antimicrob Agents Chemother. 2011;55: 3399–3405. doi:10.1128/AAC.01801-10
90. Lu C-D, Yang Z, Li W. Transcriptome analysis of the ArgR regulon in *Pseudomonas aeruginosa*. J Bacteriol. 2004;186: 3855–3861. doi:10.1128/JB.186.12.3855-3861.2004
91. Li W, Lu C-D. Regulation of carbon and ntrogen utilization by CbrAB and NtrBC two-component systems in *Pseudomonas aeruginosa*. J Bacteriol. 2007;189: 5413–5420. doi:10.1128/JB.00432-07
92. Liang H, Deng X, Ji Q, Sun F, Shen T, He C. The *Pseudomonas aeruginosa* global regulator VqsR directly inhibits QscR to control quorum-sensing and virulence gene expression. J Bacteriol. 2012;194: 3098–3108. doi:10.1128/JB.06679-11
93. Poole K, Hay T, Gilmour C, Fruci M. The aminoglycoside resistance-promoting AmgRS envelope stress-responsive two-component system in *Pseudomonas aeruginosa* is zinc-activated and protects cells from zinc-promoted membrane damage. Microbiology. 2019;165: 563–571. doi:10.1099/mic.0.000787
94. Persky NS, Ferullo DJ, Cooper DL, Moore HR, Lovett ST. The ObgE/CgtA GTPase influences the stringent response to amino acid starvation in *Escherichia coli*. Molecular Microbiology. 2009;73: 253–266. doi:10.1111/j.1365-2958.2009.06767.x
95. Belete B, Lu H, Wozniak DJ. *Pseudomonas aeruginosa* AlgR regulates type IV pilus biosynthesis by activating transcription of the fimU-pilVWXY1Y2E operon. J Bacteriol. 2008;190: 2023–2030. doi:10.1128/JB.01623-07
96. Mavrodi DV, Bonsall RF, Delaney SM, Soule MJ, Phillips G, Thomashow LS. Functional analysis of genes for biosynthesis of pyocyanin and phenazine-1-carboxamide from *Pseudomonas aeruginosa* PAO1. J Bacteriol. 2001;183: 6454–6465. doi:10.1128/JB.183.21.6454-6465.2001
97. Casilag F, Lorenz A, Krueger J, Klawonn F, Weiss S, Häussler S. The LasB elastase of *Pseudomonas aeruginosa* acts in concert with alkaline protease AprA to prevent

flagellin-mediated immune recognition. Infect Immun. 2016;84: 162–171. doi:10.1128/IAI.00939-15

98. Rao J, Elliott MR, Leitinger N, Jensen RV, Goldberg JB, Amin AR. RahU: an inducible and functionally pleiotropic protein in *Pseudomonas aeruginosa* modulates innate immunity and inflammation in host cells. Cell Immunol. 2011;270: 103–113. doi:10.1016/j.cellimm.2011.05.012
99. Goltermann L, Good L, Bentin T. Chaperonins fight aminoglycoside-induced protein misfolding and promote short-term tolerance in *Escherichia coli*. J Biol Chem. 2013;288: 10483–10489. doi:10.1074/jbc.M112.420380
100. Cardoso K, Gandra RF, Wisniewski ES, Osaku CA, Kadowaki MK, Felipach-Neto V, Haus FA, Simão RCG. DnaK and GroEL are induced in response to antibiotic and heat shock in *Acinetobacter baumannii*. Journal of Medical Microbiology. 2010;59: 1061–1068. doi:10.1099/jmm.0.020339-0
101. Okuda J, Yamane S, Nagata S, Kunikata C, Suezawa C, Yasuda M. The *Pseudomonas aeruginosa* dnaK gene is involved in bacterial translocation across the intestinal epithelial cell barrier. Microbiology. 2017;163: 1208–1216. doi:10.1099/mic.0.000508
102. Déziel E, Gopalan S, Tampakaki AP, Lépine F, Padfield KE, Saucier M, Xiao G, Rahme LG. The contribution of MvfR to *Pseudomonas aeruginosa* pathogenesis and quorum sensing circuitry regulation: multiple quorum sensing-regulated genes are modulated without affecting *lasRI*, *rhlRI* or the production of N-acyl-L-homoserine lactones. Molecular Microbiology. 2005;55: 998–1014. doi:10.1111/j.1365-2958.2004.04448.x
103. Colvin KM, Gordon VD, Murakami K, Borlee BR, Wozniak DJ, Wong GCL, Parsek MR. The pel polysaccharide can serve a structural and protective role in the biofilm matrix of *Pseudomonas aeruginosa*. PLoS Pathog. 2011;7: e1001264. doi:10.1371/journal.ppat.1001264
104. Reimmann C, Beyeler M, Latifi A, Winteler H, Foglino M, Lazdunski A, et al. The global activator GacA of *Pseudomonas aeruginosa* PAO positively controls the production of the autoinducer N-butyryl-homoserine lactone and the formation of the virulence factors pyocyanin, cyanide, and lipase. Molecular Microbiology. 1997;24: 309–319. doi:10.1046/j.1365-2958.1997.3291701.x

105. Hickman JW, Tifrea DF, Harwood CS. A chemosensory system that regulates biofilm formation through modulation of cyclic diguanylate levels. PNAS. 2005;102: 14422–14427. doi:10.1073/pnas.0507170102
106. Choby JE, Skaar EP. Heme synthesis and acquisition in bacterial pathogens. J Mol Biol. 2016;428: 3408–3428. doi:10.1016/j.jmb.2016.03.018
107. Proshkin S, Rahmouni AR, Mironov A, Nudler E. Cooperation between translating ribosomes and RNA polymerase in transcription elongation. Science. 2010;328: 504–508. doi:10.1126/science.1184939
108. Dana A, Tuller T. The effect of tRNA levels on decoding times of mRNA codons. Nucleic Acids Research. 2014;42: 9171–9181. doi:10.1093/nar/gku646
109. Goldman E, Jakubowski H. Uncharged tRNA, protein synthesis, and the bacterial stringent response. Molecular Microbiology. John Wiley & Sons, Ltd; 1990;4: 2035–2040. doi:10.1111/j.1365-2958.1990.tb00563.x
110. Tribelli PM, Lujan AM, Pardo A, Ibarra JG, Fernández Do Porto D, Smania A, Lopez NI. Core regulon of the global anaerobic regulator Anr targets central metabolism functions in *Pseudomonas* species. Sci Rep. 2019;9: 9065–13. doi:10.1038/s41598-019-45541-0
111. da Silva DP, Matwichuk ML, Townsend DO, Reichhardt C, Lamba D, Wozniak DJ, Parsek MR. The *Pseudomonas aeruginosa* lectin LecB binds to the exopolysaccharide Psl and stabilizes the biofilm matrix. Nat Commun. 2019;10: 1–11. doi:10.1038/s41467-019-10201-4
112. Dersch P, Khan MA, Mühlen S, Görke B. Roles of regulatory RNAs for antibiotic resistance in bacteria and their potential value as novel drug targets. Front Microbiol. 2017;8: 803. doi:10.3389/fmicb.2017.00803
113. Howe JA, Wang H, Fischmann TO, Balibar CJ, Xiao L, Galgoci AM, et al. Selective small-molecule inhibition of an RNA structural element. Nature. 2015;526: 672–677. doi:10.1038/nature15542
114. Mulhbacher J, Brouillette E, Allard M, Fortier L-C, Malouin F, Lafontaine DA. Novel riboswitch ligand analogs as selective inhibitors of guanine-related metabolic pathways. PLoS Pathog. 2010;6: e1000865. doi:10.1371/journal.ppat.1000865
115. Ster C, Allard M, Boulanger S, Lamontagne Boulet M, Mulhbacher J, Lafontaine DA, Marsault E, Lacasse P, Malouin F. Experimental treatment of *Staphylococcus aureus* bovine intramammary infection using a guanine riboswitch ligand analog. J Dairy Sci. 2013;96: 1000–1008. doi:10.3168/jds.2012-5890

116. Friedman L, Kolter R. Genes involved in matrix formation *in Pseudomonas aeruginosa* PA14 biofilms. Molecular Microbiology. 2004;51: 675–690. doi:10.1046/j.1365-2958.2003.03877.x
117. Buskirk AR, Green R. Ribosome pausing, arrest and rescue in bacteria and eukaryotes. Philos Trans R Soc Lond, B, Biol Sci. 2017;372: 20160183. doi:10.1098/rstb.2016.0183
118. Rodnina MV. Translation in Prokaryotes. Cold Spring Harb Perspect Biol. 2018;10: a032664. doi:10.1101/cshperspect.a032664
119. Zhu M, Mori M*, Hwa T, Dai X. Disruption of transcription–translation coordination in Escherichia* coli leads to premature transcriptional termination. Nat Microbiol. 2019;4: 2347–2356. doi:10.1038/s41564-019-0543-1
120. Davis AR, Gohara DW, Yap M-NF. Sequence selectivity of macrolide-induced translational attenuation. Proc Natl Acad Sci USA. 2014;111: 15379–15384. doi:10.1073/pnas.1410356111
121. Vázquez-Laslop N, Mankin AS. How macrolide antibiotics work. Trends Biochem Sci. 2018;43: 668–684. doi:10.1016/j.tibs.2018.06.011
122. Linares JF, Gustafsson I, Baquero F, Martinez JL. Antibiotics as intermicrobial signaling agents instead of weapons. PNAS. 2006;103: 19484–19489. doi:10.1073/pnas.0608949103
123. Gödeke J, Pustelny C, Häussler S. Recycling of peptidyl-tRNAs by peptidyl-tRNA hydrolase counteracts azithromycin-mediated effects on *Pseudomonas aeruginosa*. Antimicrob Agents Chemother. 2013;57: 1617–1624. doi:10.1128/AAC.02582-12
124. Feng B, Mandava CS, Guo Q, Wang J, Cao W, Li N, Zhang Y, Zhang Y, Wang Z, Wu J, Sanyal S, Lei J, Gao N. Structural and functional insights into the mode of action of a universally conserved Obg GTPase. PLoS Biol. 2014;12: e1001866. doi:10.1371/journal.pbio.1001866
125. Dambach M, Sandoval M, Updegrove TB, Anantharaman V, Aravind L, Waters LS, et al. The ubiquitous yybP-ykoY riboswitch is a manganese-responsive regulatory element. Molecular Cell. 2015;57: 1099–1109. doi:10.1016/j.molcel.2015.01.035

Figure 1

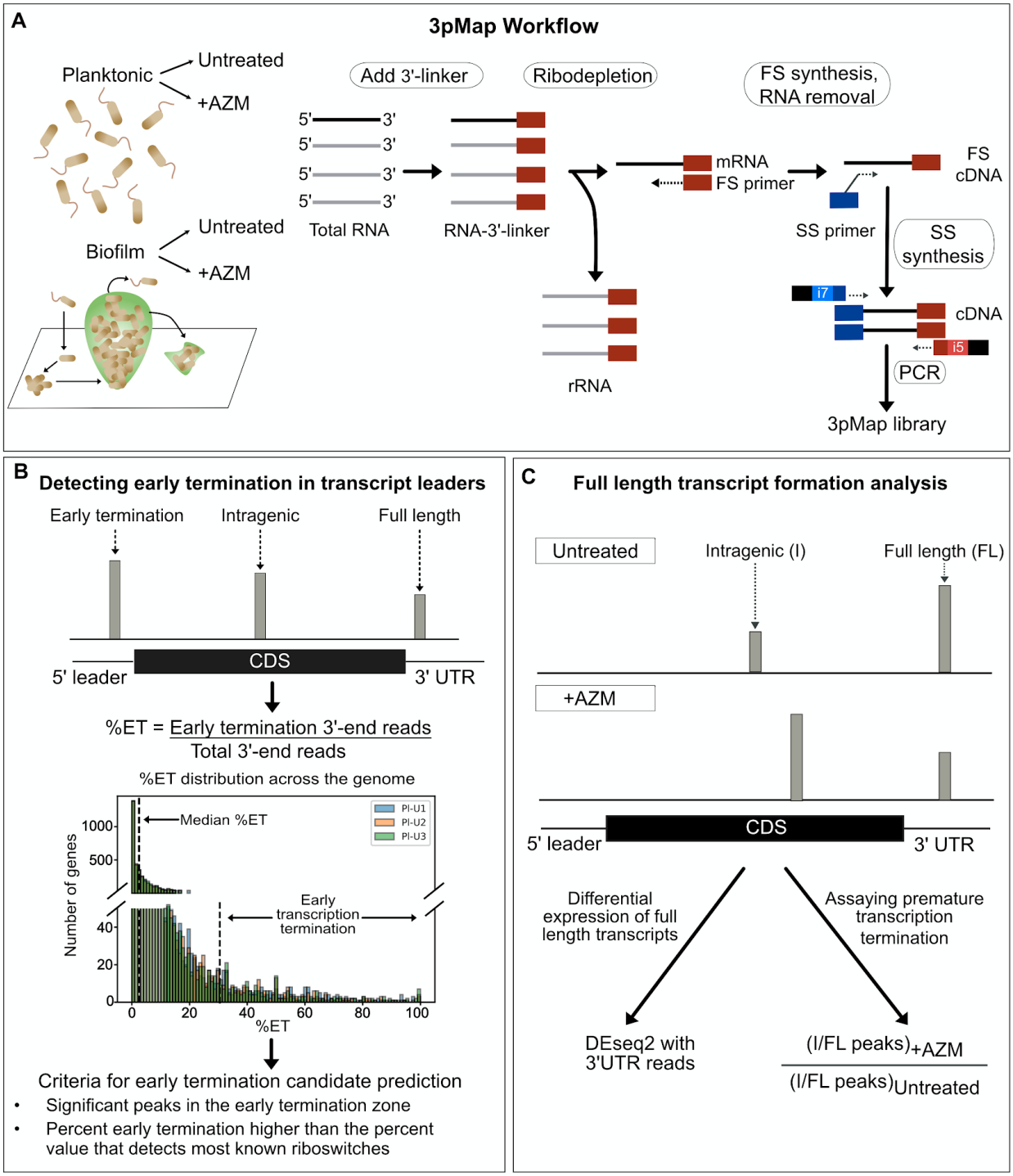
A
3pMap Workflow
Planktonic
Untreated
+AZM
Biofilm
Untreated
+AZM
Add 3'-linker
Ribodepletion
FS synthesis, RNA removal
5'
3'
Total RNA
RNA-3'-linker
mRNA
FS primer
FS cDNA
SS primer
SS synthesis
i7
cDNA
i5
PCR
rRNA
3pMap library
B
Detecting early termination in transcript leaders
Early termination
Intragenic
Full length
5' leader
CDS
3' UTR
%ET = Early termination 3'-end reads / Total 3'-end reads
%ET distribution across the genome
Median %ET
PI-U1
PI-U2
PI-U3
Number of genes
1000
500
40
20
0
Early transcription termination
0
20
40
60
80
100
%ET
Criteria for early termination candidate prediction
• Significant peaks in the early termination zone
• Percent early termination higher than the percent value that detects most known riboswitches
C
Full length transcript formation analysis
Untreated
Intragenic (I)
Full length (FL)
+AZM
5' leader
CDS
3' UTR
Differential expression of full length transcripts
Assaying premature transcription termination
DEseq2 with 3'UTR reads
(I/FL peaks)+AZM / (I/FL peaks)Untreated

Figure 1. 3pMap workflow and data analysis. (A) 3pMap library synthesis. A 3'-adapter is ligated to total RNA, followed by rRNA depletion. The cDNA is generated by reverse transcription with oligos containing sequences complementary to the adapter (first strand) and to random priming sites (second strand). The cDNA libraries are PCR amplified to generate Illumina sequencing libraries. **(B)** Predicting putative genes regulated by transcription termination. 3'-end reads are assigned to genes and categorized as early termination (transcript leader + 40 nucleotides) (ET), intragenic (I), and 3'UTR or full length (FL) reads. Genes with significant 3'-end peaks in the ET zone and %ET >30 are considered candidates for premature transcription termination. **(C)** Assaying changes in full length transcript synthesis. 3'-end reads and peaks were categorized as intragenic (I) and full length (FL) depending on their locations. Differential changes in gene expression were measured using DEseq2 of all 3'-end reads (see Methods). Relative changes in intragenic transcription termination were measured by comparing the I/FL peaks indicative of reproducible transcription stalling/stops in AZM-treated vs. untreated samples.

Figure 2

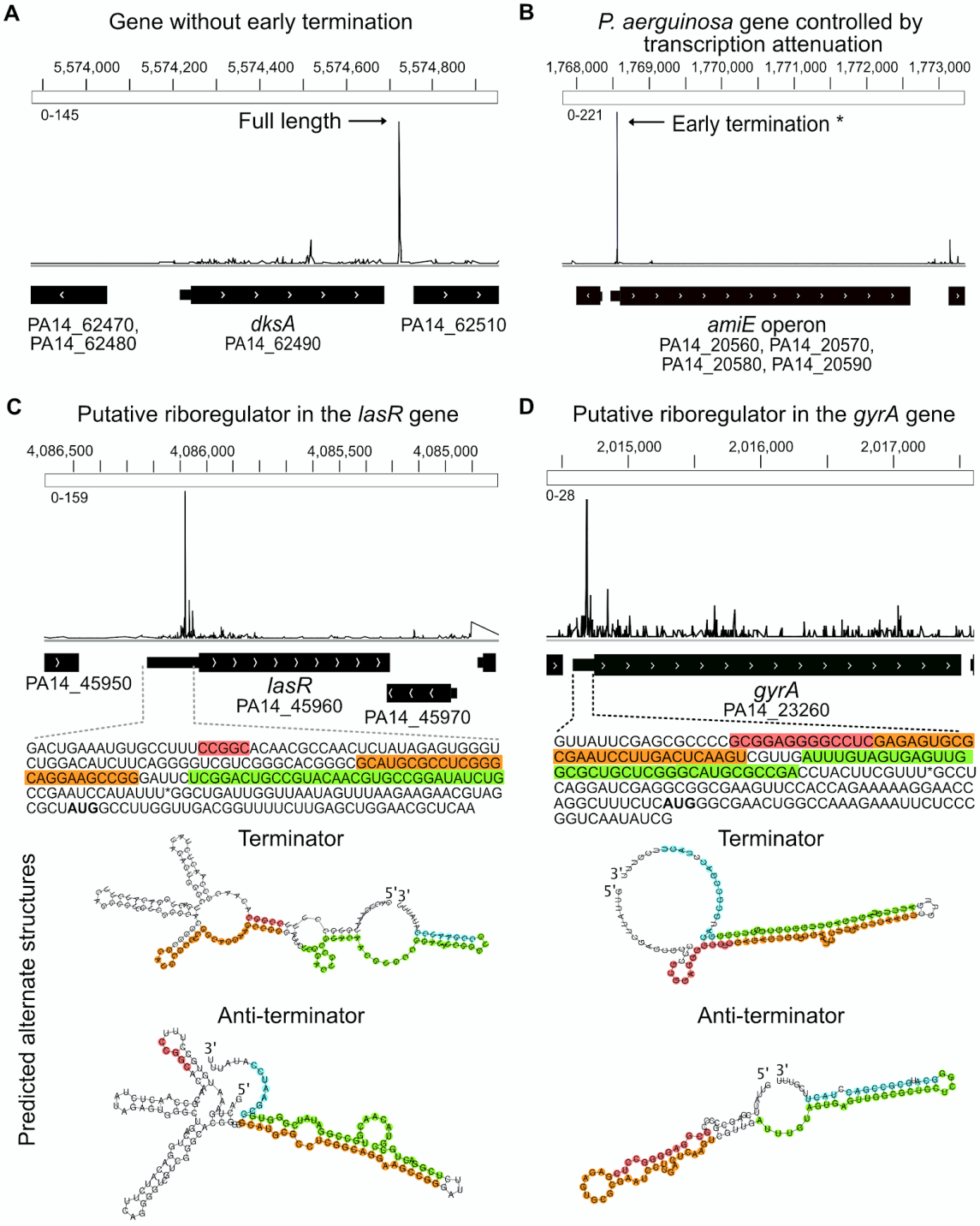
A
Gene without early termination
5,574,000
5,574,200
5,574,400
5,574,600
5,574,800
0-145
Full length
PA14_62470,
PA14_62480
dksA
PA14_62490
PA14_62510
B
P. aerguinosa gene controlled by transcription attenuation
1,768,000
1,769,000
1,770,000
1,771,000
1,772,000
1,773,000
0-221
Early termination *
amiE operon
PA14_20560, PA14_20570,
PA14_20580, PA14_20590
C
Putative riboregulator in the lasR gene
4,086,500
4,086,000
4,085,500
4,085,000
0-159
PA14_45950
lasR
PA14_45960
PA14_45970
GACUGAAAUGUGCCUUUCCGGCACAACGCCAACUCUAUAGAGUGGGU
CUGGACAUCUUCAGGGGUCGUCGGGCACGGGCGCAUGCGCCUCGGG
CAGGAAGCCGGGAUUCUCGGACUGCCGUACAACGUGCCGGAUAUCUG
CCGAAUCCAUAUUU*GGCUGAUUGGUUAAUAGUUUAAGAAGAACGUAG
CGCUAUGGCCUUGGUUGACGGUUUUCUUGAGCUGGAACGCUCAA
Terminator
5'3'
Anti-terminator
3'
5'
D
Putative riboregulator in the gyrA gene
2,015,000
2,016,000
2,017,000
0-28
gyrA
PA14_23260
GUUAUUCGAGCGCCCCGCGGAGGGGCCUCGAGAGUGCG
CGAAUCCUUGACUCAAGUCGUUGAUUUGUAGUGAGUUG
GCGCUGCUCGGGCAUGCGCCGACCUACUUCGUUU*GCCU
CAGGAUCGAGGCGGCGAAGUUCCACCAGAAAAAGGAACC
AGGCUUUCUCAUGGGCGAACUGGCCAAAGAAAUUCUCCC
GGUCAAUAUCG
Terminator
3'
5'
Anti-terminator
5'
3'
Predicted alternate structures

Figure 2. Predicting genes regulated by transcription termination in transcript leaders. IGV views show strand-specific 3'-end counts . (A) Example of a gene (*dksA* PA14_62490) not predicted to be regulated by premature transcription termination in its transcript leader. The major 3' end peak is in the 3' UTR. (B) IGV view of early termination in the *amiE* operon (known transcription attenuation) shows major 3'-end peak in transcript leader. (C) IGV view of *lasR* shows premature 3'-end peaks in its transcript leader. The sequence of the *lasR* early termination region and predicted alternate secondary structures in the transcript leader are shown below. The asterisk denotes a peak site of early termination. Alternate structures capable of early termination (terminator and transcriptional read-through (anti-terminator was predicted with PASIFIC [68] using the sequence upstream of the asterisk (corresponding to a 3'-end significant peak) as the input. (D) IGV view of DNA gyrase A (*gyrA)* shows premature 3'-ends in its transcript leader. The sequence of *gyrA* early transcription termination zone and the alternate structures predicted by PASIFIC are shown below, as in C.

Figure 3

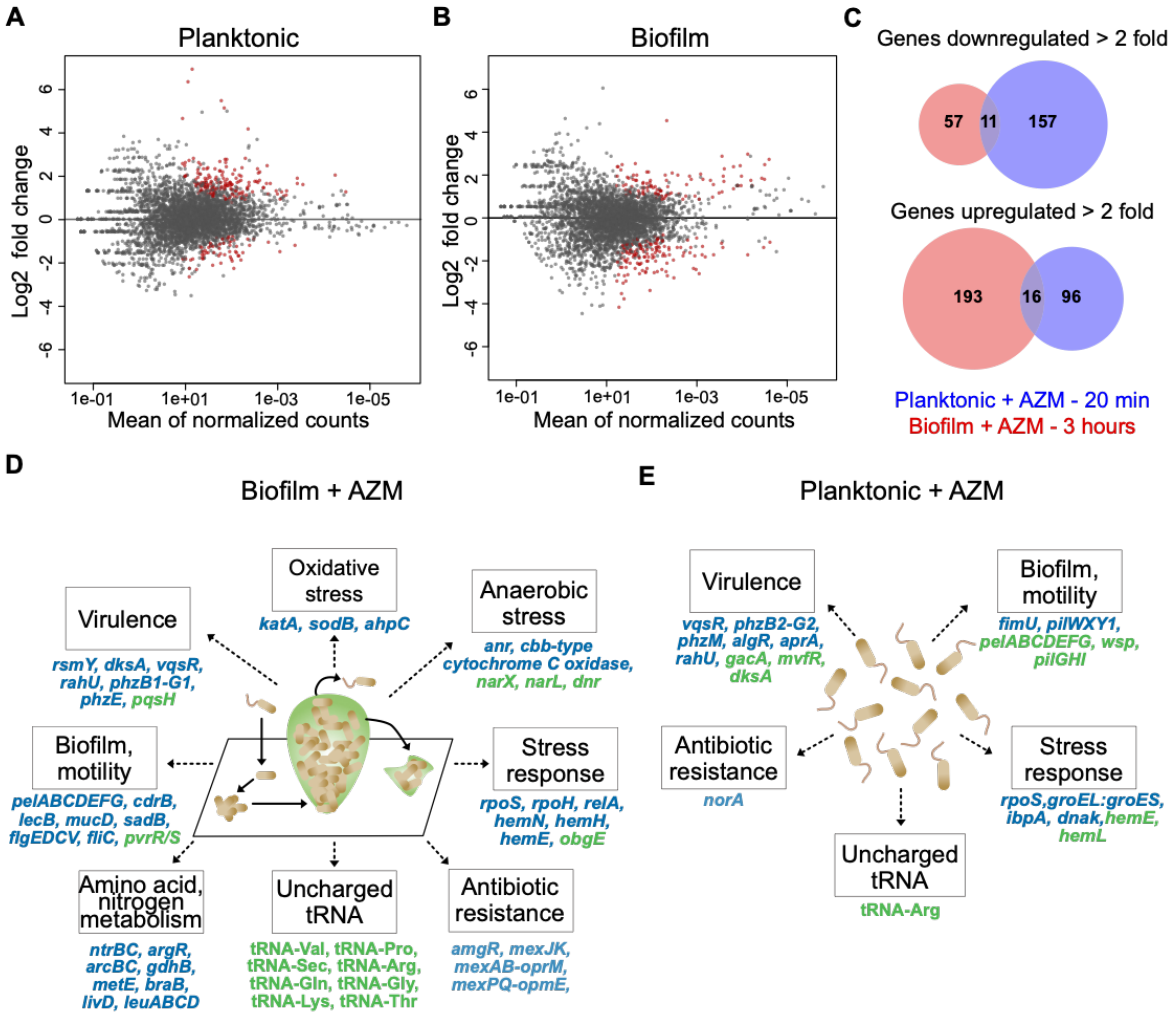
A
Planktonic
Log2 fold change
Mean of normalized counts
B
Biofilm
Log2 fold change
Mean of normalized counts
C
Genes downregulated > 2 fold
57
11
157
Genes upregulated > 2 fold
193
16
96
Planktonic + AZM - 20 min
Biofilm + AZM - 3 hours
D
Biofilm + AZM
Oxidative stress
katA, sodB, ahpC
Virulence
rsmY, dksA, vqsR, rahU, phzB1-G1, phzE, pqsH
Anaerobic stress
anr, cbb-type cytochrome C oxidase, narX, narL, dnr
Biofilm, motility
pelABCDEFG, cdrB, lecB, mucD, sadB, flgEDCV, fliC, pvrR/S
Stress response
rpoS, rpoH, relA, hemN, hemH, hemE, obgE
Amino acid, nitrogen metabolism
ntrBC, argR, arcBC, gdhB, metE, braB, livD, leuABCD
Uncharged tRNA
tRNA-Val, tRNA-Pro, tRNA-Sec, tRNA-Arg, tRNA-Gln, tRNA-Gly, tRNA-Lys, tRNA-Thr
Antibiotic resistance
amgR, mexJK, mexAB-oprM, mexPQ-opmE,
E
Planktonic + AZM
Virulence
vqsR, phzB2-G2, phzM, algR, aprA, rahU, gacA, mvfR, dksA
Biofilm, motility
fimU, pilWXY1, pelABCDEFG, wsp, pilGHI
Antibiotic resistance
norA
Stress response
rpoS,groEL:groES, ibpA, dnak,hemE, hemL
Uncharged tRNA
tRNA-Arg

Figure 3. AZM alters full length transcript synthesis of *P. aeruginosa* genes. (A and B) Scatter plot of DEseq2 analysis of expression changes in PA14 planktonic cultures and biofilms treated with AZM. Red dots indicate DEseq changes at 10% FDR. (C) Genes showing >2 fold down (top) or up (bottom) differential regulation upon AZM treatment. AZM induced regulation of planktonic and biofilm genes, indicated in blue and red, respectively, show little overlap. Key PA14 genes regulated by AZM in biofilm (D) cultures and planktonic (E) cultures. Downregulated genes are colored blue, whereas upregulated genes are colored green.

Figure 4

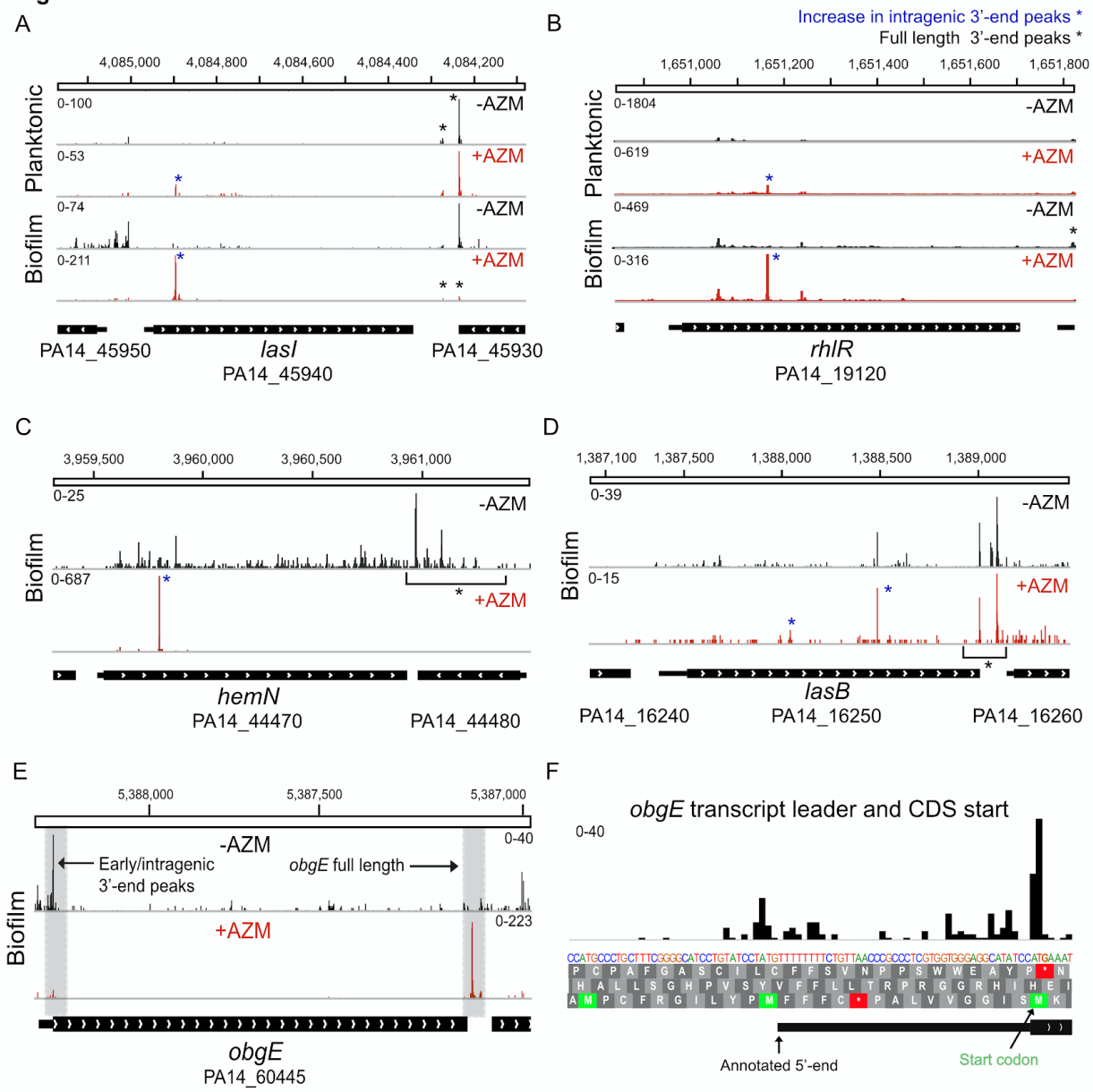
A
4,085,000
4,084,800
4,084,600
4,084,400
4,084,200
Planktonic
Biofilm
0-100
-AZM
0-53
+AZM
0-74
-AZM
0-211
+AZM
PA14_45950
lasI
PA14_45940
PA14_45930
B
Increase in intragenic 3'-end peaks *
Full length 3'-end peaks *
1,651,000
1,651,200
1,651,400
1,651,600
1,651,800
0-1804
-AZM
0-619
+AZM
0-469
-AZM
0-316
+AZM
rhlR
PA14_19120
C
3,959,500
3,960,000
3,960,500
3,961,000
Biofilm
0-25
-AZM
0-687
+AZM
hemN
PA14_44470
PA14_44480
D
1,387,100
1,387,500
1,388,000
1,388,500
1,389,000
Biofilm
0-39
-AZM
0-15
+AZM
lasB
PA14_16240
PA14_16250
PA14_16260
E
5,388,000
5,387,500
5,387,000
-AZM
0-40
Early/intragenic
3'-end peaks
obgE full length
Biofilm
+AZM
0-223
obgE
PA14_60445
F
obgE transcript leader and CDS start
0-40
Annotated 5'-end
Start codon

Figure 4. AZM alters intragenic 3'-end peak formation in PA14 genes. (A and B) AZM dependent increase in intragenic premature 3'-end peaks in *lasI* and *rhlR* genes. IGV views of *lasI* and *rhlR* in control (-AZM) and AZM treated (+AZM) treated samples from planktonic and biofilm cultures are shown. Intragenic peaks whose relative levels are altered by AZM are indicated with blue asterisks. The *lasI* gene in planktonic cultures and biofilm showed ~16 fold and ~41 fold increase in I/FL peak ratio upon AZM treatment, respectively. AZM treatment resulted in an ~8 fold increase in I/FL peaks for *rhlR* in biofilms. The peak is not prominent in planktonic cultures. (C) IGV view of the *hemN* gene downregulated by AZM (DEseq2 $\log_2$fold change = -1.2) shows a 60 fold increase in I/FL peak ratio. The effect is less pronounced in planktonic cells (D) IGV view of *lasB* downregulated by AZM (DEseq2 change = ~1.95) shows moderate increase in I/FL ratio (1.74 fold) in the presence of AZM. (E) 23 fold upregulation of *obgE* (is accompanied by a 42-fold reduction in transcription attenuation in its transcript leader. (F) A closer view of the transcript leader and CDS start shows termination before the rare codon for Lys at the *obgE* start codon.

Figure 5

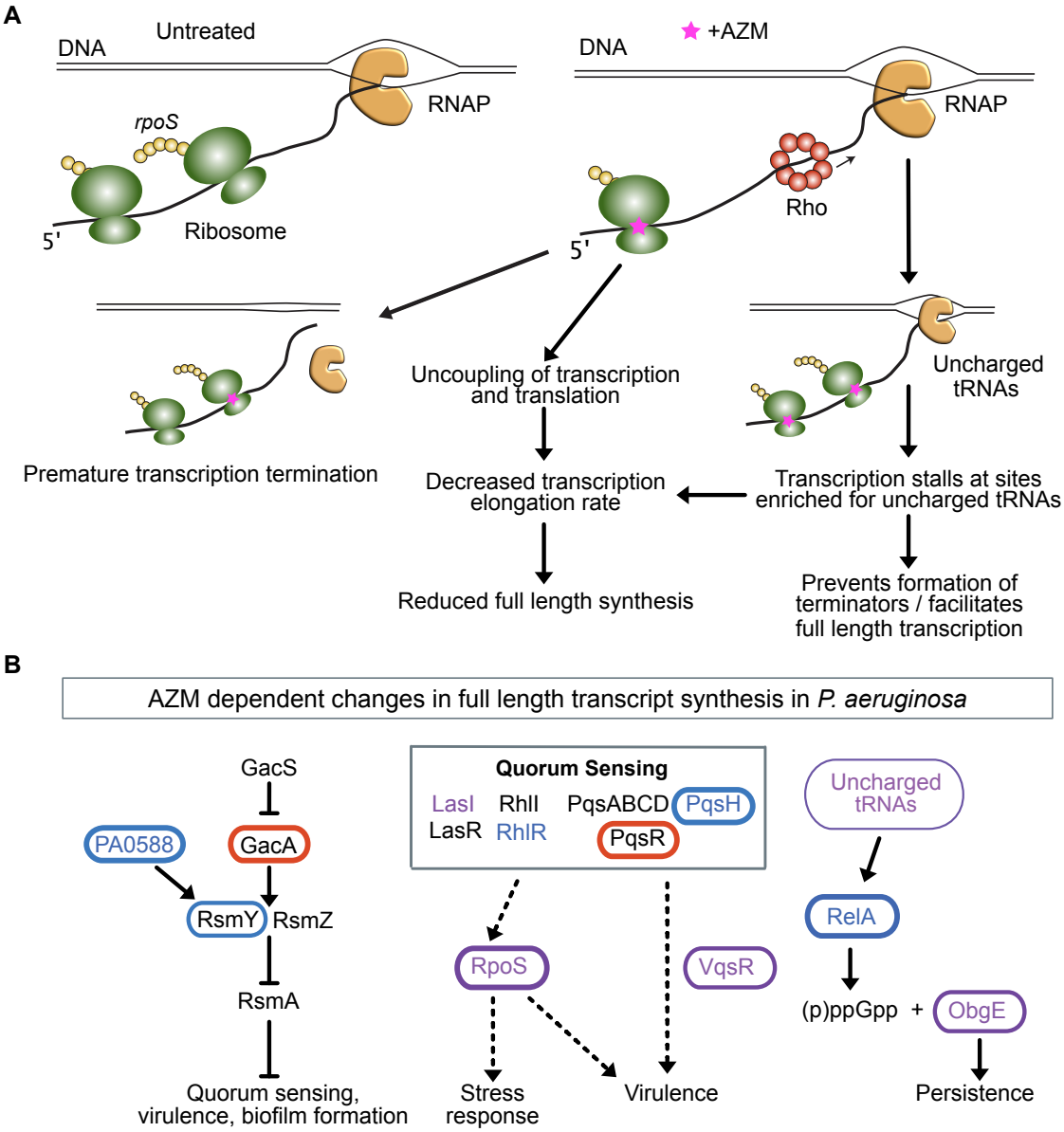
A
Untreated
DNA
RNAP
rpoS
Ribosome
5'
+AZM
DNA
RNAP
Rho
5'
Premature transcription termination
Uncoupling of transcription and translation
Uncharged tRNAs
Decreased transcription elongation rate
Transcription stalls at sites enriched for uncharged tRNAs
Reduced full length synthesis
Prevents formation of terminators / facilitates full length transcription
B
AZM dependent changes in full length transcript synthesis in P. aeruginosa
GacS
PA0588
GacA
RsmY
RsmZ
RsmA
Quorum sensing, virulence, biofilm formation
Quorum Sensing
LasI
RhlI
PqsABCD
PqsH
LasR
RhlR
PqsR
RpoS
VqsR
Stress response
Virulence
Uncharged tRNAs
RelA
(p)ppGpp
+
ObgE
Persistence

Figure 5. Model of *P. aeruginosa* response to azithromycin. **(A)** Azithromycin induced translational stalling uncouples transcription and translation, leading to premature termination and the accumulation of uncharged tRNA. Premature transcription termination directly decreases the expression of many genes, including primary transcriptional modulators like *rpoS* (shown). Translational stalling and the accumulation of uncharged tRNA could induce expression of the ribosome rescue GTPase *obgE*, which dissociates 70S subunits [124]. **(B)** Impact of AZM on gene expression of key *P. aeruginosa* regulators. Network diagram depicts several genes found to be differentially regulated and exhibit premature transcription termination within the GacS/GacA signal transduction system, quorum sensing systems, and stringent response regulators. These genes, and their regulons, have been shown to be highly interconnected, therefore only a subsection of interactions are shown here. Oval outlines indicate that a gene was differentially expressed upon AZM treatment as detected by DESeq2. Significant hits for altered relative I/FL ratio upon AZM treatment is shown by color of the text. Genes with altered expression or early transcription termination in biofilms are indicated in blue, in planktonic culture in red, and in both conditions in purple. The nature of the expression changes are indicated in Figure 3D.

TABLES

Table 1. Genes predicted to form alternate structures by PASIFIC [68] or Rho-independent transcription terminators [69] in their early transcription termination zone. Comments of low confidence and very low confidence indicate PASIFIC Scores < 0.5 and < 0.3, respectively. Genes with known riboregulators are indicated in bold. Percentage early termination values are provided in the supplementary table S2.

Gene	PA14 gene product	Sequence of the early termination zone (transcript leader + 40 nt of the CDS). The sequence used to predict alternate structures by PASIFIC is shown in bold. * indicates 3'-peaks detected in the early termination zone. Start codons are shown in red. Intrinsic terminators are indicated in blue (for stem sequence) and green (for loop) colors. Reference for riboregulation of the gene is included, if applicable .
PA14_19130	autoinducer synthesis protein RhlI(rhlI)	**ATGTGTGTGCTGGTATGTCCTCCGACTGAGAGGGCCCAGG AGTATCAGGGTAGGGATGCCGCCTTTTTTTT*CTCGGCCGG CACGACACGGGGACTTGGTCA*TGATCGAATTGCTCTCTGA ATCGCTGGAAGGGCTTTCCG*CC** Note: Alternate structure predicted with full ET sequence. Regulation by transcription attenuation [76].
PA14_28360	hypothetical protein	CCGGACCCGACCGATCGGGTTGTCGC**GACGGGCATGGAG GGGTGATCGGTCGGTCGGGTTCGCGTCT*TTTCGGGGCACC CGAATCTGAAAAAATCTTGCTTCTCGCCATACCGGGGGAG CGGGGCGGGTAGATTTT***CTTCCGAATCCTTCACTTTCTACC CGGTCATGGA*AAAAGCTCTGAAATTGGCGTCATGCCTCTAC GGCC
PA14_28250	secreted acid phosphatase	GCTGTACATCCCTGGATCCTTTCCCGGCCTGCTCCACGCGG CCGGGATTTTTTT*GCCCG*CCGCAGCCGCTTCCCGGACAAC GCGTCAATCGGTTACGTCATTGC*GCCATCGCGATTGTGGTA CCGCAC*GCCTTGAAGTATGAAAACACACCGCCAT
PA14_40430	hypothetical protein	**GCTTTGCAGTTCATCGGAGTTGGCTTTCATTCGTGACTCCA GGGCAATCATTGCCGAAGCATAGCGATGTTTTCGGCAAGG ACTGAAGAGGCAC*GCGT*GCCCGCAGGAGGTTTTCA***TGC CCGGCCACCGCATCACCCTCACCGGAGAAAAGCAGA
PA14_20560, PA14_20570, PA14_20580, PA14_20590	acylamide amidohydrolase(amiE), chaperone, aliphatic amidase expression-regulating protein(amiC), aliphatic amidase regulator(amiR)	**ATCAGGTCATGCGCATCAGCGTCGATGTCGCGGGACCGAA CCTAACGCATACGTACAGAGCAAATGGGCTCTCCCGGGGT TACCCGGGAGGGCTTTTTTCG***TCCCGAAAAAATAACAACAA GAGGTGATATCCATGCGTCACGGCGATATTTCCAGCAGCAA CGACACCGTCG Note: Low confidence score

PA14_39970	phenazine biosynthesis protein(phzA2)	**CTGTCAAATCTGGTTACAACTGGGTTTCAGGCGAAACATTC GGTCATGGCAATTCGGCATTAGTTGAAACTTTGGAGACGCT CCGAAGCGGGCAACTTTT***GCCCGGAAAAAGTTTCACGGCA ATTTCTCCGGCCTGTCATCCCGATGTCTTCTTTCCGGTATGG ATGCCAGTCGATTCGAACTGGCGGAGATTCGCACCATGCGA GAGTACCAACGGTTGAAAGGGTTTACCGACAACC Note: Low confidence score
PA14_49480	hypothetical protein	**ACCATTAGTAGCGCTGTGCCACCACATGGATTGTTGGGGA AGCGATAGAAAGACCGAAGCCCCGCCTTGTGCGGGGTTTT TTATT***GGAATGAAAATGCAAATAACTAAACTAACCCTCCATC GCTTTAAAAAAT Note: Very low confidence score
PA14_12560	hypothetical protein	**CTGTTTCAGTTGTCATGCCCGCGTGGCCCCCGCATATAAAG AGCAGCCTGCTCGTAGAACGATAAACGCCTTGCCCGCCCC CCATGGCACGCTCCGTCCGACCGCGAGCCGGACTTCGTTT*** GCTTGAAAATCCGGAGGTTGCCAATGGATCCCGAACTGTTC GAAGAGTGGATGATGACCGGTC
PA14_61260	hypothetical protein	**TCGCTGTAGCGGGCCGTCTGCAACCCAGTCCCCTCTCCGG CAGACCATGAGGT*GCCTACCCGCGCCGAAAGTTACACCC T*GCTTCGCGTTACCTCGCGCTGGGTGGAAGAGC*TCCGT*A ACACCAGGCGCCCTTCCAAGTTT*GCTCAAT***CGGCAGTTGA CGTAGCCGGTGACTACCGTC*ACCCATGCTCTGCC*GGGCA GCCAACC*GAATTTCGGTCGCCCGCCCCT*GGGTGGCCGTA TAGCGTTCTAGAGGTGAAAACGTGGAGCTT*TTATCAGGCGC TGAAATGGTCGTCCGCTCGT Notes;yybP-ykoY manganese riboswitch in PAO1 homolog [125]
PA14_26420	TonB-dependent receptor <u>PAO1 cobalamin</u> riboswitch (RFAM)	**AATCCAGATCGTTCAAGGCTTGACTGGAAACGGTGCGGAT GTTCCCATCCGGCCCGTTCCAGGTGCCTCCTGCCGCCGCG CAGGAGGTGAAACGGGAAGCCGGTGCGTCACTTCAGTGAT CAGTCCGGCGCTGCCCCCGC*AACGGTAAGCGAGCGAAAT CCTCTTCAGGCCACTGTGCTCCAGCATGGGAAGGCGAGGA TTTCACGA*CCCTCGCAAGCCCGGAGACCGGCCTGCAACG CCCTGTTGGCACACCCGCGGTGGGCGGGAGCGAGCCGGT TGTTCGAGGCGCTGTCGC*GCCTGCGATTTCCTGC***GCGTTC CGTCCTGCCCGGTCATGAGATGGAACGCCCATGCCCCGCTT CAGCCGTTTGCGCACCGAGCCTTTCGCCC
PA14_21650, PA14_21660	hypothetical protein, hypothetical protein	ACCGGCCTGCCTGCCGAAGTACGTTGGACCCCACAAGAAG CCTCGCTCATTTGCGAGGCTTTTTGCTTTTCCGGCCTCGCG CCCTGTGCTAGAAGGCTGCCTCTGCGAGTCCGTTCTGTTCT GGAGTACCCCT0GTGGAGTCTGAATCCATCGTCTATGGCTG CATCCGCGACT
PA14_00080	hypothetical protein	**GGCAATGGAATGGCAATCCCAGGCCAGGGAGTCATTTGGC ACGCAGCAGTGGGTGTCTCGGAG*TACGTGCGAACCCCTT GGCGGGTGGATCACCG*GAGTAACGCAGTAAGCGCCTA*TC GCA*TGCCAGCACGGCCGACCGGCCGT***GTTTCCACC*ACA GGTGGAGCGGGCATGACGACGGGGAGT*TCCGGGGC*GTC TGCCCGTTCCCAAGGACGGTA*ACCGTGAAACGCCTGAAAA AGACACTGCACCTTTCAAGCTTGT

PA14_69190	transcription termination factor Rho(rho)	**CGCGACGTTTTTTCCGTCGCCTTCTGCATGCCGTCCCGGAC GCACTTCCTACTCGAACTTT*CTAGCGCTCCTGTCGCCCCCT TGCGACACGGCTTT***CCCAAGCTCGACGCTTTCTCCAATTCC TCTTTCTGCGTACCTATCTCTTT*CCTATGAATCT*GACCGAA CTCAAGCAAAAGCCGATTGCCGAAC Note: Very low confidence score (highly confident with unknown 3'-end specified on PASIFIC input)
PA14_42870	hypothetical protein	**CTGTCAAATCTGGTTACAACTGGGTTTCAGGCGAAACATTC GGTCATGGCAATTCGGCATTAGTTGAAACTTTGGAGACGCT CCGAAGCGGGCAACTTTT***GCCCGGAAAAAGTTTCACGGCA ATTTCTCCGGCCTGTCATCCCGATGTCTTCTTTCCGGTATGG ATGCCAGTCGATTCGAACTGGCGGAGATTCGCACCATGCGA GAGTACCAACGGTTGAAAGGGTTTACCGACAACC*GCGGCT GAACATCCGCCA*TCGTCGCCGGAAAGCGGCGTCACCAGTG GTCCCGACAGGACAGGAAGGAAATGAACCTGATCGCGCAC GTGGAAATACCGGTGTCCGACC Note:Low confidence score
PA14_01290, PA14_01300, PA14_01310, PA14_01320	cytochrome c oxidase subunit II(coxB), cytochrome c oxidase subunit I(coxA), cytochrome C oxidase assembly protein, cytochrome c oxidase subunit III(coIII)	**GAATGCTGAACCTGATGAACCCGGCCTGCCTTGCTGTGTG CCGAGGTGCGACGGTCAAAGT*TCGTTGTCTTGGCGGTCCA CCCCTTGGCCGTT*GGCGTCTGCCGGC.GGGATAAAAACAA CGATAAGGGGAACCCGA*ATGCTGC*GACATCCACGAGTCT GGATGGGCTTCCTTTT***GC
PA14_59380	hypothetical protein	**GTGATCTGCTGACGTTGTCAGCGACATGCCCCCATGCAGC TCGGATCCGAAATGCTGCAGCACAGCCCACCGTGTTGATC CAACCCAAGACCGCATAGCTTCTGGTAGCGCGGTCGGTCG GCCTCGGTCGATAGAAGCTCCC*TTCCGCAACCCAGCGGG GAATCCACTTCCCCGCCAGGGCCAGTGTTTT***CTCCGCACC CTCAACCTGCAGGAGAAACACCATGTCCAAGCAATCCACCA GCTTCGAAATCGGCTTTGCCC Note: Very low confidence score
PA14_10740	spermidine acetyltransferase	**TCCGCCGGATGCTCGGCCAGTCGAAGGGAGGAACGAAGC ATGTCGTATGAACAGTCCAGCAGCGTACCTAGCGACTTTCT TTCCTCCTTTTTCCA***AGAGCCTGTCATCCATGATCGAACTCA GAACCATCACCCGCGACGACTGGGAAA
PA14_02450, PA14_02460, PA14_02470	NAD(P) transhydrogenase subunit alpha part 1, NAD(P) transhydrogenase subunit alpha part 2, pyridine nucleotide transhydrogenase subunit beta(pntB)	TTTCTATGTCGTATGCCTTCAGAACTTGTTGAAGGCTTTTCG GCTCGATTGCACAATGCCGCGCCAAGGTTCGTTCGCGAATC GCGGTATGTGAGCTAGACCTCCGCAGCCGGTGCGCCATCC GCAGTGCCCCGGACTACTCGACAATCACGCAGGAGATTCGT GAGTGCAGATCGGTGTCCCCCTCGAGACCCATGCCGGTGA GA
PA14_57580, PA14_57590	30S ribosomal protein S9(rpsI), 50S ribosomal protein L13(rplM)	**GCCTTTCATCGGTGGGGGATGCCAAGCCTGCCGATCGATG TATCTAGTCGTTACGGACGCACACC*GACCCGAGCCCCAAT TCGTGTCTGTTTTCGGCT***GTCCTTGACTT*GTCAAGGCAACC ACTGTCCAGTAAGATTCGCC*GTCTTATTTTCAGGCGGCCCC TGAGGCTAT*AACGAATGAAAACCTATACCGCGAAACCGGAA ACTGTACAGCGCG Note: Very low confidence score

PA14_45960	transcriptional regulator LasR(lasR)	**GACTGAAATGTGCCTTTCCGGCACAACGCCAACTCTATAGA GTGGGCTGACTGGACATCTTCAGGGGTCGTCGGGCACGGG CGCATGCGCCTCGGCAGGAAGCCGGGATTCTCGGACTGCC GTACAACGTGCCGGATA*TCGGGT*GCCGAATCCATATTT***GCTGATTGGTTAATAG*TTTAAGAAGAACGTAGCGCTATGGC CTTGGTTGACGGTTTTCTTGAGCTGGAACGCTCAA
PA14_27050	Slt family transglycosylase	**CTGGAATTCGCAGCGAGGCGGCGCCCCCTCGATCGCGCC GGACCCGCCGGGGGATGGGTGGCAAACCGCTTGTAGAAC AATCCGTTATAATCGCAGATCGGGTTCTTCGGC*GCCCGGA TTATCTACCCAATGCCTCCGTTTGCAGCCGCTGTCGGAGAG GAACTTGCCAAGACT*GCCATGCTCTGATTGATCCGGTCCC CCGGAGAGGGACATCGA*GCCTGGCCTCT*GGAGACCTGG ATGACGCGTCTGTTGCTGCTTTCGCTTT***GCCTGCTGGT*GC
PA14_21020	non-ribosomal peptide synthetase	**GCTCTTGCTTCGGGTGCCGCCGCTTCCCTGCCAACCACGCT GGCTACGGCGCGCTGAAACGT*CGACGGGT*GGAACCTGT CCGGCGAGGCGTGCGGT*GCCCGTGTTCGCCGAATCGATG GATTGTTGAAGAGGACGCAGGGATGGTTCGTTTC***GCTCGC TTGCCGCTATCGCCCTACCAAC Note: Low confidence score
PA14_30050	isocitrate lyase	**GCTCCCGCTAATCAGGGGCTCTGAAACGACGAGCTCCCGG TGCCTGCGCCGATACGCCCTCGGCCTCCACCGTGTT*GATC TGCCCACAAGGCGGCTTGACGAGATTGCGACT*GGAACGA AGTTGTCCTGAGGGACGGGGAAGCGTTT***ACGTATCAGCCA GATCGAAAGACTCGACAGCGAGTCGCCCACCGGCAACCAC GAGCCGAACGGCACTTGA*TCCAGTCGAGAAGCACGGTCCG CGAACTGT*TCGTCTCCACCCCCTCCTCGGCGTCATTCTTCG CCACGGTCATTCTCTCGCCATGCAGCGGTGAGCCACCCG*C AAGACAACCTTCACCAGCAGGTTTTGAGTGGGTCAGTCGGT GCTCAACCAATACATTTCTTGAAGGATTGACCATGTCCGCAT ATCAGAACGAGATCAAGGCAGTTGCCGCGC
PA14_00990	hypothetical protein	**AACCTTTCGAGTCATCCGATATTCATCAATGGCTCCTACAA GATCCGACG.GAGTGGATCTTACAAGCGAAGGTGAGGGCC GCGCAGC*GGCTCCGATGATAGGGAGA.TCGTCACCGTGCT GGATGTACCCGTTT*TGCT***GGCCGCCGTATCCCCGG
PA14_44170	hypothetical protein	CTTTCGCGTTGGAGCGGCACGACATCCGCCGTTTGTCACGG CGGTTTCATCTGCGCTCCCTAGACTGCCGATAAACCTGATG AGGAGACGGGCAATGAATTCGCAACACACCGATACCGCCAA GCGCCGCGTGA
PA14_62150, PA14_62160	acetolactate synthase 3 regulatory subunit(ilvH), acetolactate synthase 3 catalytic subunit(ilvI)	**TCGCTGTAGCGGGCCGTCTGCAACCCAGTCCCCTCTCCGG CAGACCATGAGGT*GCCTACCCGCGCCGAAAGTTACACCC T*GCTTCGCGTTACCTCGCGCTGGGTGGAAGAGC*TCCGT*A ACACCAGGCGCCCTTCCAAGTTT*GCTCAAT***CGGCAGTTGA CGTAGCCGGTGACTACCGTC*ACCCATGCTCTGCC*GGGCA GCCAACC*GAATTTCGGTCGCCCGCCCCT*GGGTGGCCGTA TAGCGTTCTAGAGGTGAAAACGTGGAGCTT*TTATCAGGCGC TGAAATGGTCGTCCGCTCGT
PA14_31150	hypothetical protein	AGTGCCCAAAAATCGCTGTTCCGTGCTTTTACGGAAATCCGC ATTTACGGATTTCCACAGAACCGGGGAATCGCATCCGTGTC TTTCCGGCTTCCTGCAATTGCGCTTCTGCGCTTTCGTTCTTC TACGGATGCGATGGCTTGTGCATCCGTGTTTCCACACGCAT GCACGGTTCCGTGG

PA14_10750	sugar efflux transporter	**ATTCGGCAGTTCCCTCCAATACCTATAACGACCATCCAACG CACATCGCCGCCCCGGACCCTTGCGTCCGGGGCGTTTTCC GTC***GTGCGTGGCGAGGGTCGCGGGACCTGCCCGTCCGCC CCCTGCTCCGGAACCGAACGCCCCATGGACAGCACCTCCG AAACCCGCAGCGGCAGCTGGCTGA Note: Very low confidence score
PA14_NovelOrf_001	PA14_NovelOrf_001	**GACAATTCAGTGGTTTGATGGGATCTGACGGGGAGCTTTCT AAGTTGCCCAGTGGGAATTACGAGGCCTCCTG*TTCAAAAA GAGCGGCGGCAGTTGGGAGGCTCGAGTGAGCTTTCACTC*** ***GCC*CGCAACAGCGGCTGGATCTTCGCC*GTCATCGCCACT CACTGAGCCTGACAGCTTT***TTGCTATGCTGCCGACCTGCG CCG*TGGGACTTAGTTGGCACCGGC
PA14_16020	hypothetical protein	**ACCGACGAAAGACCGTCGTCACCCTATCCAAGGTTGGGTG ACAAACGAAGCCCACGAAGAGGATGATTGCATCTAGCCAT CATCCTCTTTTTTCA***TCAGGCCATGACCATGTCCAATCAACA ACATTCCCGCCTGGGCCAGA Note:Very low confidence
PA14_30200	cold-shock protein CspD(cspD)	**ATACCCCTACAGGGTATCAGGGGTTCCGCACCCGTCTCGA CCCAGGTCGGACGCGGGATCGTAGT*GGATGATACTCCAG CGTTGGAGTCCTTTGC***AGAGGGATATGAGCAT*GCTCAGCG GTAAGGTCAAGTGGTTCAACAACGCCAAGG Note: Low confidence score
PA14_28770	hypothetical protein	GCGGCGGTGATTTTCATTGCATGGTGGACTGACGCGAATTT TGGGGGGTTACAGCAGGGGCACTGCAATGATGTATGACTGA GAACTTTTTGAATAAAATGGTTCTTTTTTTATATCTTGCTACG CTAGGCAGAAACTGAATAAGAGCTGCTGGCAACAGAGGTTG AAACGTGACATGGGTTGATTGTTGGGGTATTGCAATCAGGA CGCGTCGGTACGATATGCCAACATATATATATCGTCTCTGGG AGCAACGAATGGATAATCTGAAAACACGAATCGTCAATTCAT ACAATG
PA14_62400	aminotransferase	**AAGAAAGCGCCTGGCTGGTGCTTTCCAGGCCGCCGCAGCG GCCGGCGTCGCTCGGACGGTTCCGGGCGCTTACGTTACTC CGAGGACAGCATGGCTGAATCACGCCCTGCGCGCCGTTTC GCGC***GCATC
PA14_64520	bacterioferritin	GTAAGCAGAAAAAGCCGGCCGCAGAGCCGGCCCTTTTCACC GGATCAGCCTCAAGGAGAAAACCG**ATG**ACCACCGTTCAACT GACGGACGTCCAGACCCTTCGCG
PA14_58150	rod shape-determining protein MreB(mreB)	**ACTTTTTTACCCGCGTATTTTTCACCCACGCTTCGCCTAGGG TTTCTTTCCCATG*TTCAAAAAATTGCGTGGCATGTTTTCCA GC***GATCTGT Note: Very low confidence score
PA14_NovelOrf_009	PA14_NovelOrf_009	AGTATGTAGCCGGCTAATTTCCCCGGCTGGGGAGATTGCTG TTATGGAAATGTCCACCTTAAGGGGAACACG-ATGAACAACGTTCTGAAATTCTCTGCTCTGGCTCTGGCTG
PA14_19100, PA14_19110	rhamnosyltransferase chain A(rhlA), rhamnosyltransferase chain B(rhlB)	**ATCGGCTACGCGTGAACACGGACGCCAATCGTTTGCGCAG GCCGATCTGCAAGACCCACACAAGCCCCTCGCCTGAAGGG GTACGCATCCGCCGT*GGCTGGTCCGCGCGGATGGCCGCT* GAGT*TACTTGTCTGCCGTTCGAACAATAAGAACGAACTCT ACGTAATGCCGGGATACCCGTGGCAGCGATAGCTGTTT***GC CTGTTCGAAAATTTTTGGGAGGTGTGAGATGCGGCGCGAAA GTCTGTTGGTATCGGTTTGCAAGGGCC Note: RNA thermometer known to regulate *rhlA* [76].

PA14_09490	phenazine-specific methyltransferase(phzM)	**TCCTGCAATGCCGGAGGTTGTAGCCAAGTTGTAATTTTATT CTTTCGGTACGCAGGAAAAGGCTCTGGAACAGGCAGTTGG AAAGTTCCAGGGTTGTTTCCGCAACGAGATCCAGGGAGCG CTGATCCGGGGGATGAGCGCATTTTTC***TCAAAGTTCCGAAT GAACCGGGGTGTTCTGCGGTATTTCTCGCCGAACGGGCAAG AAGTGCGAAATAGAGCGCTTGGGTACTTCTC*GGGTTACGG AAATGTGTAACGAGAGAGAATAAAAGATGAATAATTCGAATC TTGCTGCTGCGCGTAATTTGATAC
PA14_21710	hypothetical protein	**CTGCGTGAGCGCGGACGGCCCCGGCGGCCGGCT*GTCCGT TCATCGTAGCCGGTTTCGGCTGCGGCACTAAACGCGGCCG CTACGCTCTGATGGGAGCGGAGTTTTGCGT***CGATGTCGAG GAGGGCGCCCATGTTCAAGCCGCTACCGATCA
PA14_23590, PA14_23610	transcriptional regulator, hydrolase	TTTTTCCCGCTCTGCGGGGCTCTATAGGGCCATTCCGAATT GGAATGGCCCTTTTGTTTTTTCCCTTTTCGAATTTCCTGACAG ACGGTCCGGCCGTACGCTTGCCGATTTTTATTATGCATATAA TATTTCACTCATAATATTTTCGGAGATCGTCATGAGCGACAA GAAAACCCAGACCCGTGCCCGCATCCTCG
PA14_23260	DNA gyrase subunit A(gyrA)	**GTTATTCGAGCGCCCCGCGGAGGGGCCTCGAGAGTGCGC GAATCCTTGACTCAAGTCGTTGATTTGTAGTGAGTTGGCGC TGCTCGGGCATGCGCCGACCTACTTCGTTT***GCCTCAGGAT CGAGGCGGCGAAGTTCC*ACCAGAAAAAGGA*ACCAGGCTT CTCATGGGCGAACTGGCCAAAGAAATTCTCCCGGTCAATAT CG
PA14_05820	hypothetical protein	**GCAACACCCCGGCGCGCTTTTTCACGGTAGCGCGCCGGCC GCCGGGGAGACGGGCAAGGAACCCGTCTT***CCCGGCCATT TCCGTTTC*CAGCCCCCAGCAGCGAGAACCGTCATGCCCGG CGCCCTTTCCCATATCCGCGTACTCGACCTGT Note:Low confidence score

SUPPLEMENTARY FIGURES

Supplementary Figure 1.

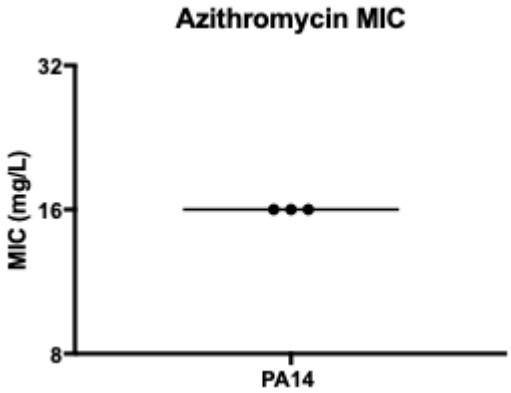

Supplementary Figure 1. The MIC of AZM was determined by broth microdilution according to CLSI guidelines [S1]. Three replicate assays were performed. Briefly, twofold microdilutions of Azithromycin dihydrate (Fisher J66740) in Mueller Hinton Broth were inoculated with $5x10^5$ CFU/mL PA14 in a 96 well plate. After 16-20 hours of incubation at 37ºC, MIC was determined to be the lowest concentration of antibiotic at which no visible growth was observed.

Supplementary Figure 2

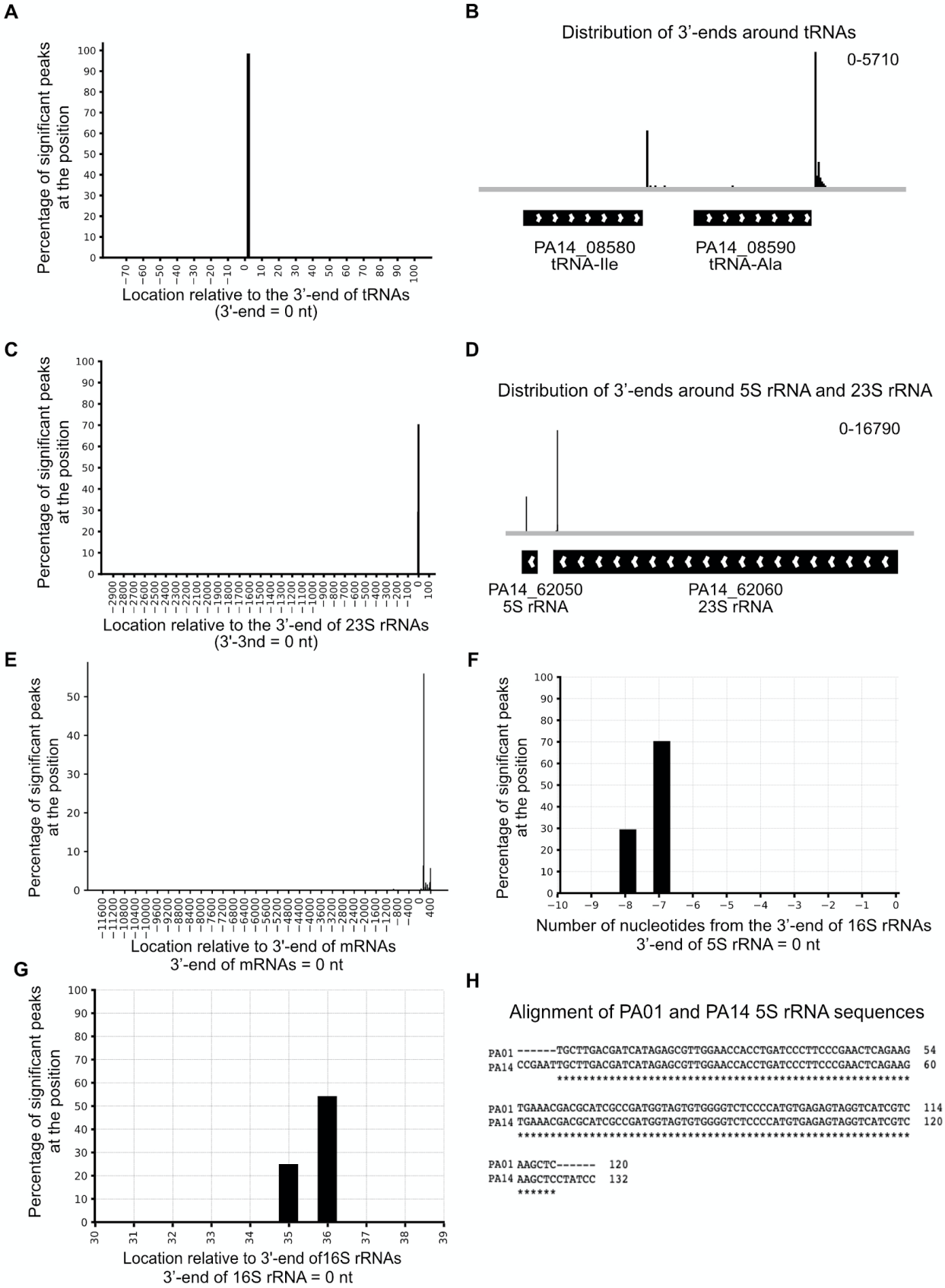

Supplementary Figure 2. Genome-wide mapping of RNA 3'-ends in planktonic cultures of PA14 using 3pMap. **(A).** Location of 3pMap reads with respect to the 3'-end of tRNAs (RNA end = 0 nucleotide). 98.78% of the significant peaks within or downstream of tRNAs are located within 3 nucleotides from the annotated RNA ends. **(B)** Genome browser view of distribution of 3'-ends around two tRNA genes in a planktonic untreated sample. Number of 3'-end reads corresponding to each sample are denoted on the top of the sample tracks. **(C)** Location of 3pMap reads with respect to the 3'-end of 23S ribosomal RNAs. 99.8% of the significant peaks within or downstream of 23SrRNA genes are located within 3 nucleotides of the annotated RNA ends. **(D)** Genome browser view of the distribution of 3'-ends around representative 23S rRNA and 5S rRNA genes. **(E)** Location of 3pMap reads with respect to the 3'-end of CDSs. RNA 3'-end = 0 nucleotide. 88.4% of significant peaks associated with mRNAs were located in intergenic regions, with <12% located within coding sequences. **(F)** 99.9% of RNA 3'-end significant peaks associated with 5S rRNAs were located -8 or -7 nucleotides upstream of their annotated RNA ends. **(G)** Extended 16S rRNAs in *Pseudomonas aeruginosa.* 80.54% of the detected 16S rRNAs (<10,000 reads in three replicates) had RNA 3'-ends in +35 and +36 nucleotides downstream of their annotated RNA 3'-ends. **(H)** Alignment of 5S rRNA sequences from PA01 and PA14 genome annotations using Clustal Omega (www.ebi.ac.uk). The 3'-end identified by 3pMap matches with the annotated PA01 5S rRNA 3'-end.

Supplementary Figure 3

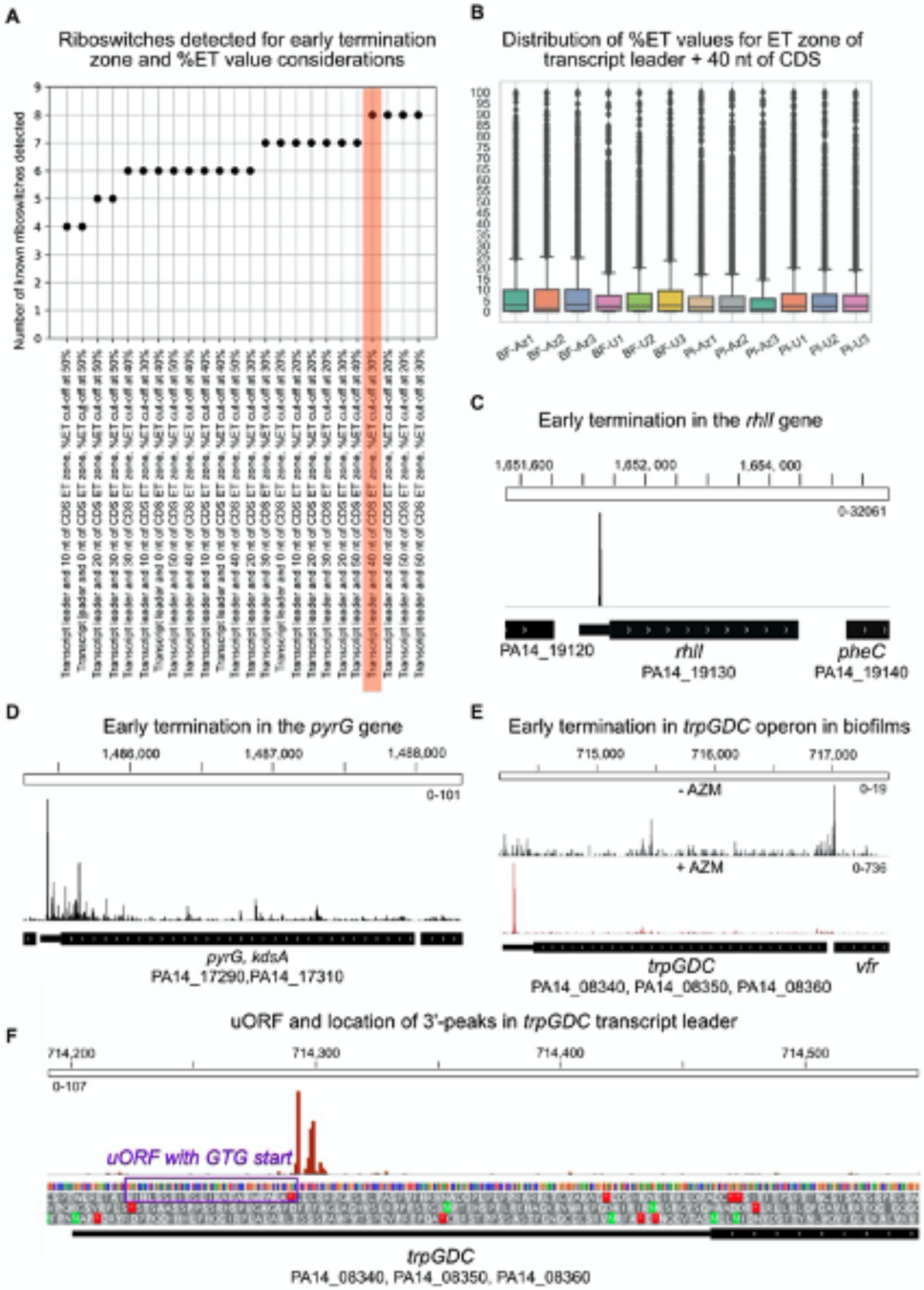

Supplementary Figure 3. **Early Termination in PA14 transcript leaders. (A)** Determining the early termination zone. Number of known riboswitches reported on Rfam detected for each ET zone and %ET cut off considerations. The lowest ET zone consideration of transcript leader + 40 nt in CDS and the highest cut-off value of 30% detected 8/11 riboswitches reported on Rfam, and was therefore used for predicting putative riboregulators. **(B)** Box Whisker plot showing the distribution of %ET values in samples using ET zone transcript leader + 40 nt of CDS. **(C)** Early transcription termination in the *rhlI* gene detected by 3pMap [S2]. Genome browser images show strand-specific tracks for the strand same as the gene of interest and in untreated planktonic samples unless specified. **(D)** Potential regulation of the *pyRG* gene by in *P. aeruginosa* by early transcription termination. The *pyrG* expression is controlled by transcription attenuation in *B. subtilis* [S3]. Genome browser image shows *pyrG,kdsA* operon. **(E)** Predicted regulation of the *trpGDC* operon by early transcription termination in *P. aeruginosa* biofilms. %ET values in planktonic (untreated and +AZM) and untreated biofilm samples were below the cut-off value. However, in AZM-treated biofilms (+AZM), regulation by premature termination was predicted. The gene is predicted to be regulated by transcription attenuation in *B. subtilis* [S4]. **(F)** A closer view of the transcript leader and early termination peak in *trpGDC* operon. The 3'-end peaks are located adjacent to a potential uORF with GTG start codon.

Supplementary Figure References

S1. CLSI. Performance standards for antimicrobial susceptibility testing. Wayne, PA: Clinical and Laboratory Standards Institute; 2019.
S2. Thomason MK, Voichek M, Dar D, Addis V, Fitzgerald D, Gottesman S, Sorek R, Greenberg E. A rhlI 5′ UTR-derived sRNA regulates RhlR-dependent quorum sensing in *Pseudomonas aeruginosa*. mBio. 2019;10: 43. doi:10.1128/mBio.02253-19
S3. Turnbough CL, Switzer RL. Regulation of pyrimidine biosynthetic gene expression in bacteria: Repression without repressors. Microbiol Mol Biol Rev. 2008;72: 266.
S4. Du H, Tarpey R, Babitzke P. The *trp* RNA-binding attenuation protein regulates TrpG synthesis by binding to the *trpG* ribosome binding site of *Bacillus subtilis*. J Bacteriol. 1997;179: 2582–2586. doi:10.1128/jb.179.8.2582-2586.1997